FINAL PROJECT REPORT

Project Title:

DEVELOPMENT OF NANOBIOCOMPOSITES BASED ON CELLULOSE NANOFIBRILS FROM LIGNOCELLULOSIC MATERIALS FOR ADVANCE ENGINEERING APPLICATIONS

Grant No.:

1001/PTEKIND/814133

Project Leader: PROF. DATUK DR. ABDUL KHALIL SHAWKATALY

Co-Researcher: ASSOC. PROF. AZHAR ABU BAKAR

RESEARCH ACTIVITIES

No	Objective	Research Findings Summary	Time Involved	Achieved
1	To study the fundamental properties (viz. Physical, morphological, mechanical, chemical and thermal) of empty fruit bunch fibres	- Physical, morphological, mechanical, chemical and thermal properties of empty fruit bunch fibres have been studied	Aug 2011 – Jan 2012	Done
2	To isolate the nanocellulose fibres by chemo-mechanical process from empty fruit bunch fibres	- Cellulose has been extracted by soda pulping and bleaching process - Cellulose microfibre has been treated by acid hydrolysis - Nanocellulose has been successfully produced by High Pressure Homogenizer	Feb 2012 – Jan 2013	Done
3	To study the properties of nanocellulose and fabricate high performance nanobiocomposites for advanced engineering applications	-Morphological, chemical, crystallinity and thermal properties of nanocellulose have been studied - Fabrication of nanobiocomposites have been done	Feb – July 2013	Done
4	To study the fracture surface morphology, mechanical and thermal properties of nanobiocomposites	- Morphological, mechanical and thermal properties of nanobiocomposites have been studied	Aug – Dec 2013	Done

DEVELOPMENT OF NANOBIOCOMPOSITES BASED ON CELLULOSE NANOFIBRILS FROM LIGNOCELLULOSIC MATERIALS FOR ADVANCE ENGINEERING APPLICATIONS

ABSTRACT

The aim of this study was to investigate properties of cellulose nanofibril (CNF) from oil palm Empty Fruit Bunch (EFB) fibers. The method of cellulose nanofibril preparation was included pulping, bleaching, acid treatment and high pressure homogenization. The fiber's properties were characterized using X-ray diffraction (XRD), Fourier Transform Infrared spectroscopy (FTIR), scanning electron microscopy (SEM), transmission electron microscopy (TEM), atomic force microscopy (AFM), thermogravimetric analysis (TGA) and differential scanning callorimetry (DSC). According to XRD results, the crystallinity index in cellulose nanofibril increased from the raw fiber to treated fiber. The FTIR analysis revealed that the pulping and bleaching processes eliminated the lignin and hemicelluloses from the fibers. The SEM analysis revealed that the diameter of fibers decreased from raw to cellulose fibers. The width of cellulose nanofibril obtained by this process was around 5 nm. The thermal stability of cellulose nanofibril was higher than other samples. In addition preparation of nanobiocomposites with 0.5% of cellulose nanofibril showed increasing mechanical and thermal properties, which make these nanobiocomposites as promising materials for engineering applications.

Keywords: Cellulose Nanofibrils, High Pressure Homogenizer, Nanobiocomposites

PEMBANGUNAN BIONANOKOMPOSITE BERDASARKAN SELULOSA NANOFIBRILS DARIPADA BAHAN LIGNOSELULOSIK UNTUK APLIKASI KEJURUTERAAN TERMAJU

ABSTRAK

Tujuan kajian ini adalah untuk menyiasat sifat-sifat selulosa nanofibril dari gentian kelapa sawit kosong Buah Tandan (EFB). Kaedah penyediaan selulosa nanofibril telah dimasukkan pulpa, pelunturan, rawatan asid dan penyeragaman tekanan tinggi. Hartanah Serat dalam setiap langkah telah disifatkan menggunakan pembelauan sinar-X (XRD), Spektroskopi (FTIR), mikroskopi pengimbasan elektron (SEM), penghantaran mikroskopi elektron (TEM), daya atom mikroskopi (AFM), analisis Termogravimetri (TGA) dan pembeza imbasan callorimetry (DSC) untuk. Menurut keputusan XRD, indeks penghabluran meningkat daripada serat mentah untuk dirawat satu dan kemudian menurun pada selulosa nanofibril. Analisis FTIR mendedahkan bahawa selepas pulpa dan proses pelunturan lignin dan hemiselulose disingkirkan daripada gentian. Berdasarkan analisis SEM diameter gentian berkurangan daripada mentah serat dirawat asid. Lebar nanofibril selulosa didapati dengan proses ini adalah sekitar 5 nm. Juga kestabilan terma daripada selulosa nanofibril adalah lebih tinggi berbanding sampel lain. Selain penyediaan nanobiocomposites dengan 0.5% daripada selulosa nanofibril menunjukkan peningkatan sifat mekanikal dan haba yang membuat nanobiocomposites ini sebagai bahan-bahan yang menjanjikan untuk aplikasi kejuruteraan.

1. Introduction

Oil palm is one of the most economical perennial oil crops in Malaysia. It has reported that Malaysia alone produced about 40 million tons oil palm annually. Oil palm biomass represents abundance availability, inexpensive and readily available source of lignocellulosic biomass (Jonoobi et al., 2011a). Many studies have been conducted on the cellulosic sources of isolated nanofibres such as oil palm (Fahma et al., 2010, Fahma et al., 2011, Nazir et al., 2013, Haafiz et al., 2014), wood pulp (Siddiqui et al., 2011), kenaf (Jonoobi et al., 2009, Jonoobi et al., 2010, Jonoobi et al., 2011a, Chan et al., 2013), bamboo (Yu et al., 2012), flax (Qua et al., 2011), rice straw (Lu and Hsieh, 2012) and etc.

Nowadays, extensive attentions have been paid to extraction of cellulose especially in nano-size due to its abundance, renewability, low cost high mechanical properties and etc. This nanosize cellulose can be generally divided into two categories, cellulose nanowhisker (CNW) and cellulose nanofibrils (CNF). The first one which can be produce using acid hydrolysis process has rod-like shape and low aspect ratio while the second one known as CNF has high aspect ratio and can be prepared by mechanical processes such as homogenization (Siqueira et al., 2010). In homogenization process cellulose suspension pass through very small nozzle and high pressure is applied to reduce fiber size into nano scale. There are many investigations related to production of CNF from various cellulosic fibers (Bhatnagar and Sain, 2005; Henriksson et al., 2008; Li et al., 2012, Jonoobi et al., 2009; Jonoobi et al., 2010; Karimi et al., 2014). There are a few studies have been studies conducted on the isolation of CNF from oil palm EFB fibers. So, it seems necessary to develop researches about production of CNF from oil palm EFB fibers using homogenization process.

One of the most important applications of CNF is in nanobiocomposites. Nanobiocomposites are materials which at least one of their components has nano-zise. Various types of nanobiocomposites films using different polymers have been prepared from homogenized CNF (López-Rubio et al., 2007; Alemdar and Sain, 2008; Jonoobi et al., 2012). However, there is lack of knowledge about production of CNF with epoxy matrix (Lu et al., 2008; Masoodi et al., 2011). The present research aims to explore the preparation of CNF through high pressure homogenizer and to evaluate the effect of CNF on properties of oil palm EFB fiber-epoxy composite.

2. Experimental

2.1 Materials

Oil Palm EFB (OPEFB) fibres were obtained from Malaysian Palm Oil Board (MPOB), Kajang, Selangor, Malaysia. The chemicals used in this study were analytical grade and obtained from Mega Makmur Scientific Sdn. Bhd. (sodium hydroxide (NaOH), sodium silicate ($NaSiO_3$) and hydrogen peroxide (H_2O_2)) and Chembumi Sdn. Bhd. (magnesium sulphite (Mg SO_4) and H_2SO_4), Penang, Malaysia.

2.2 Methods

The details methodology for the isolation and characterization of nanofibril from oil palm empty fruit bunch is presented in Figure 1.

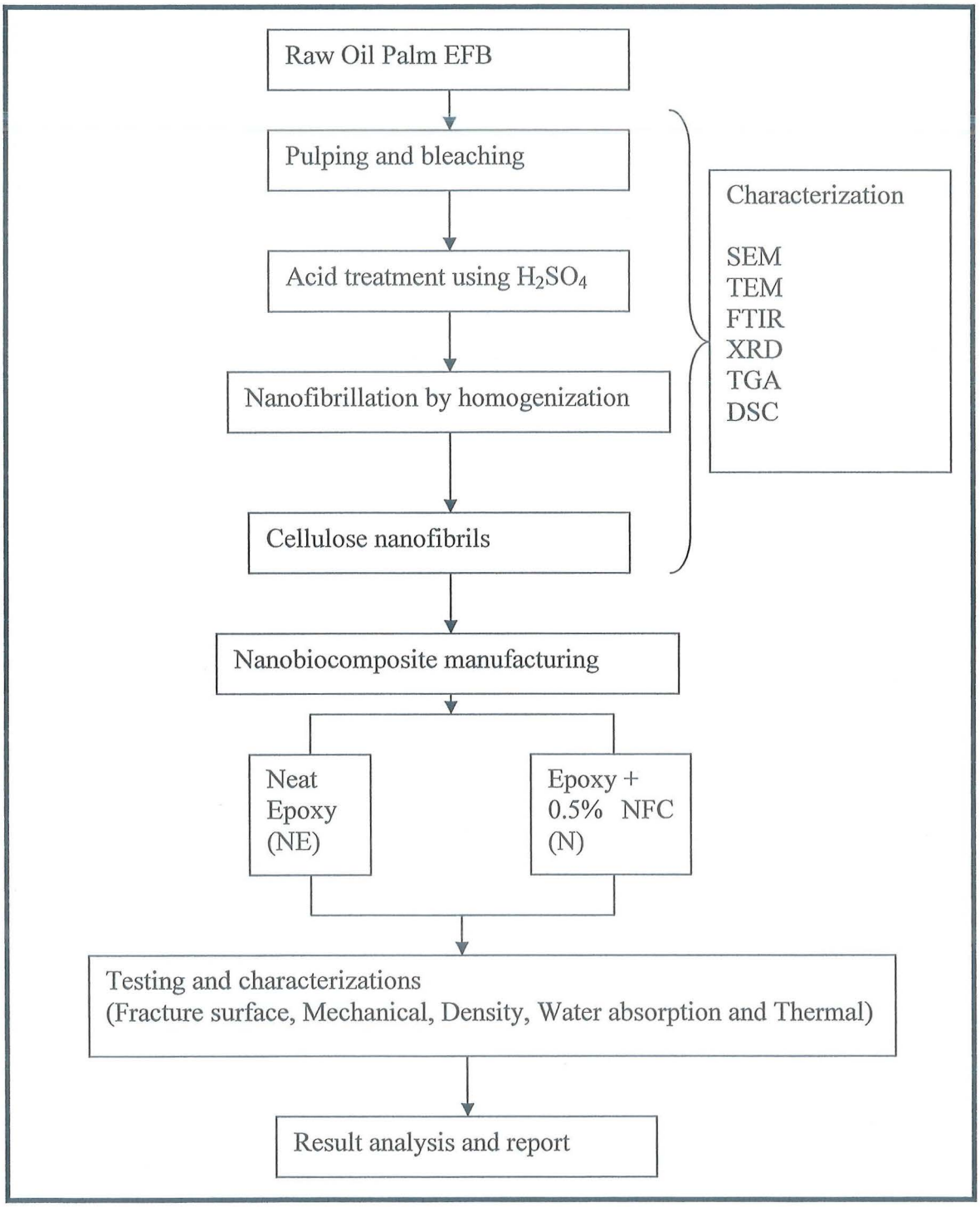

Figure 1: Flowchart for the isolation and characterization of nanofibril from oil palm empty fruit bunch

2.2.1 Raw Fiber Analysis

EFB fibers were cut to the length of 2-3 cm, air dried and grounded into fine particles. In order to obtain homogenous samples, the fibers were sieved through 100 mesh screens to eliminate the fine and coarse fibers. The ensuing EFB fibers were characterized for morphological, mechanical, chemical and thermal properties. Figure 2 shows the process of raw oil palm empty fruit bunch fiber analysis.

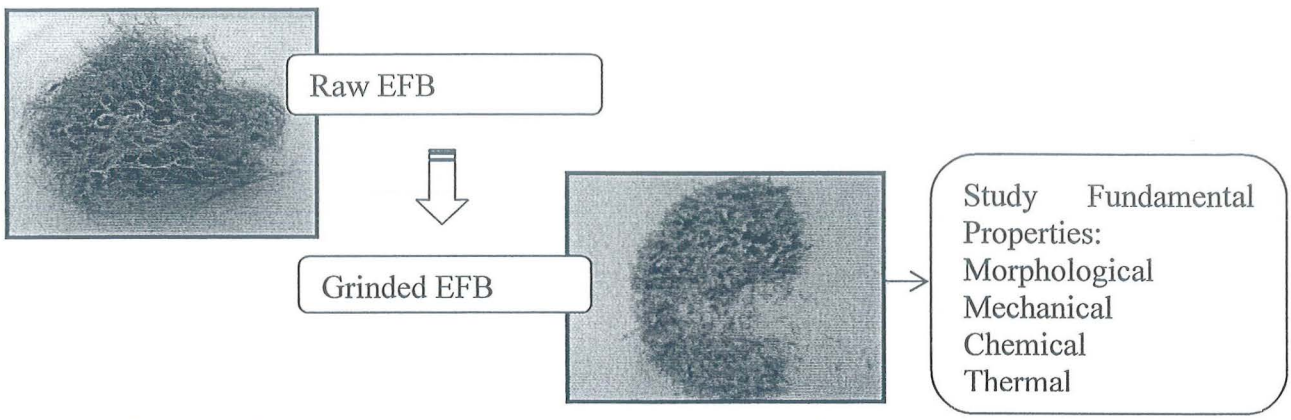

Figure 2: Process of raw oil palm empty fruit bunch fibers analysis

2.2.2 Pulping Process

Pulping was carried out in a stationary stainless steel digester. Active alkaline NaOH was added to the grinded oven dried EFB. Pulping was done with liquor to material ratio of 7:1. The heating time was 90 minutes to reach 160°C and retained the temperature for 120 minutes. The ensuing pulp was oven dried for at 60°C for 24 hours. Figure 3 represents the oil palm empty fruit bunch pulp.

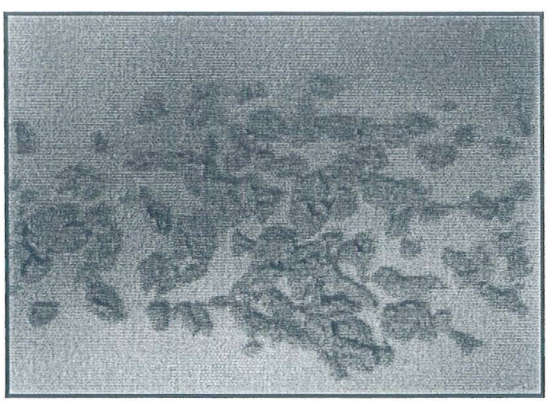

Figure 3: Oil palm empty fruit bunch pulp using NaOH.

2.2.3 Delignification Process

The chemicals and reagents used in the bleaching process were 0.039M magnesium sulfate, 0.33M sodium hydroxide and 35% hydrogen peroxide. The slurry was heated at 80°C for 2 hours. Finally, the collected slurry was washed and dried at 60° C for 24 hours in the oven. Figure 4 shows the bleached oil palm empty fruit bunch pulp.

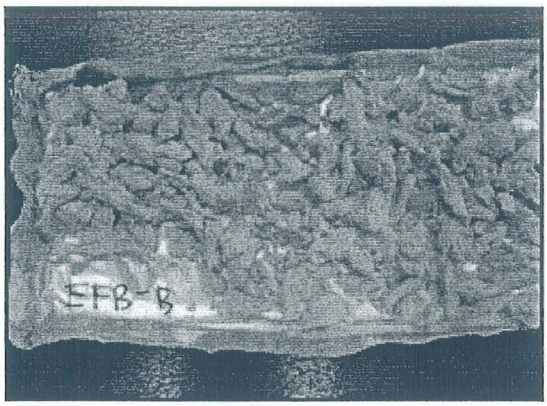

Figure 4: Oil palm empty fruit bunch bleached pulp

2.2.4 Acid Hydrolysis Process

Acid hydrolysis of the bleached pulp was conducted using 60% H_2SO_4 at 45° C for 1 hour. The acidic suspension of cellulose microfibers was neutralized by washing with distilled water. The details acid hydrolysis process of OPEFB bleached pulp is shown in Figure 5.

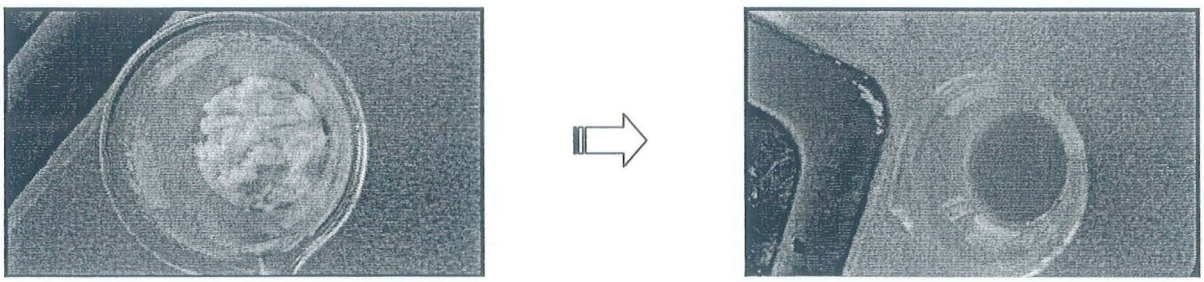

Bleached OPEFB pulp
Before chemical treatment

Bleached OPEFB pulp
After chemical treatment

Figure 5: Chemical treatment process

2.2.5 Nanocellulose Production

Figure 6 shows the nanocellulose production process from OPEFB. The cellulose microfibre undergoes a pre-treatment with mechanical disintegration before the homogenization process. The pretreated cellulose microfibrils were used to produce cellulose nanofibrils by high pressure homogenizer. Finally, the slurry was dried for characterization.

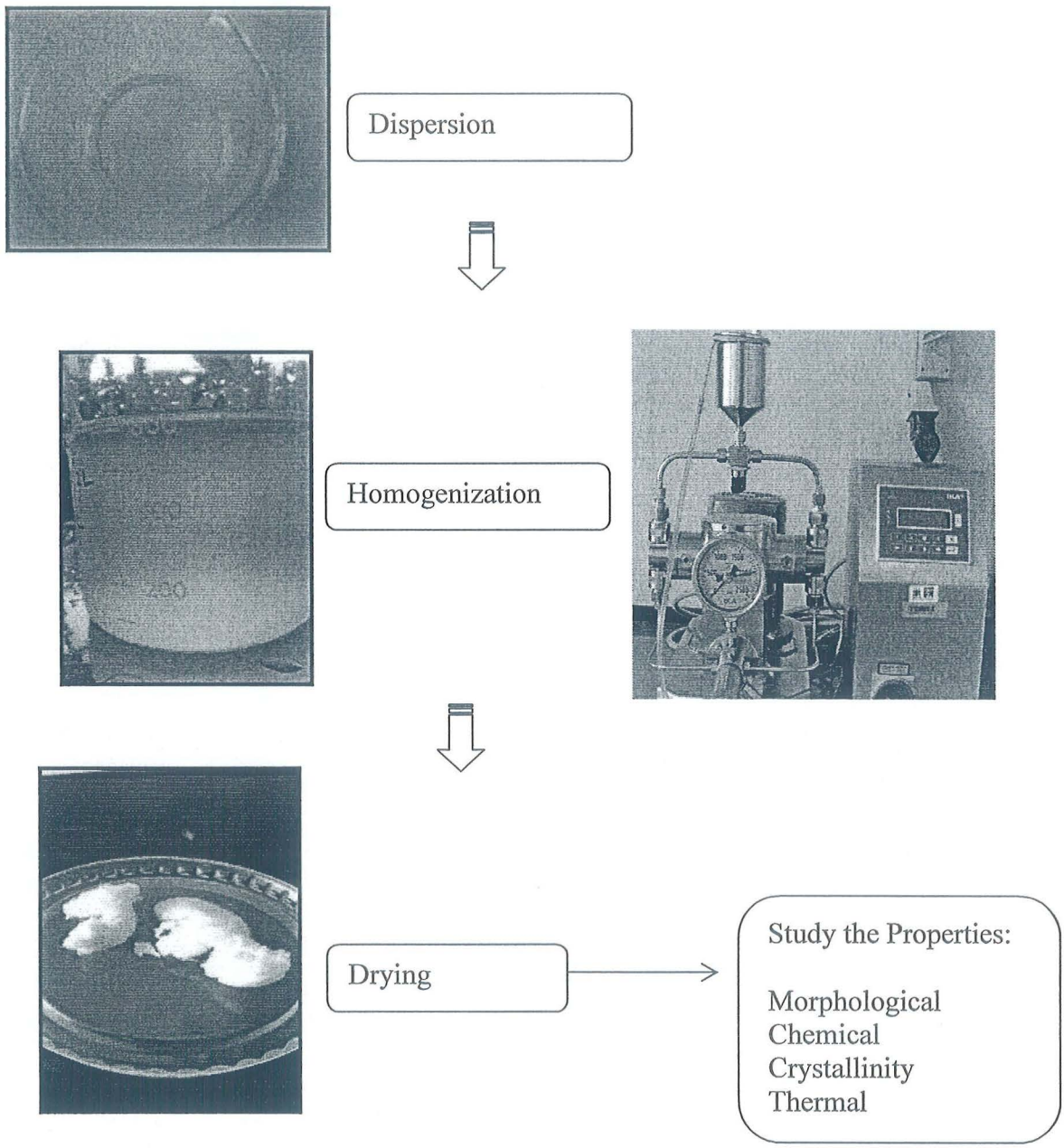

Figure 6: Process for the nanocellulose production from oil palm empty fruit bunch

2.2.6 Nanobiocomposite Fabrication

Nanobiocomposite was fabricated using 0.5% of CNF and epoxy resin. The dimension of mould used was 160 mm × 160 mm × 3 mm. The epoxy resin was mixed with 10% diluents (benzyl alcohol) and blended with 0.5% of CNF for 30 minutes using mechanical stirrer. Then the polyamide curing agent was added and mechanically stirred for 10 minutes. Later the mixture was vacuumed in vacuum chamber. Finally, the mixture was casted into mould and left to cure at 105°C for 1 hour in hot press. After cured, the nanobiocomposite was removed from the mould and post cured in oven at 105°C for 30 minutes. The nanobiocomposite fabrication process is presented in Figure 7.

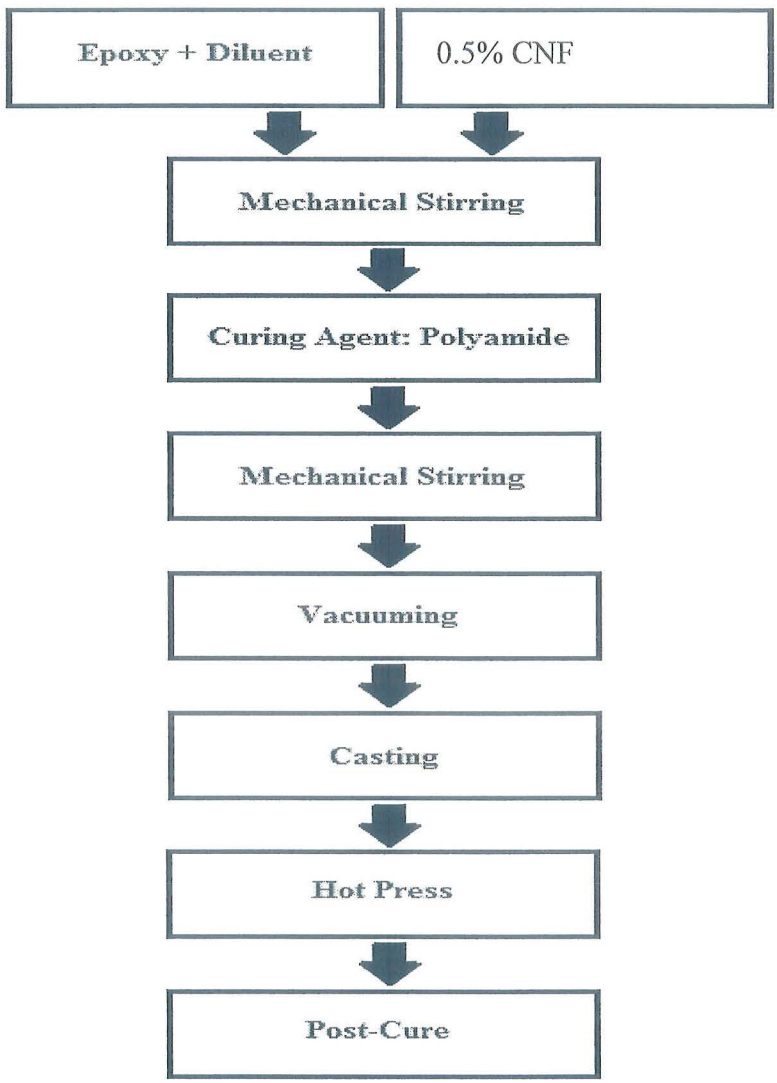

Figure 7: Flowchart for the Nanobiocomposite Fabrication

2.3 Characterization

2.3.1 Morphological characterization

The morphology and size of raw and cellulose fiber was studied by Field emission scanning electron microscopy (ESEM) (model: Leo Supra 50 VP, Carl-Zeiss SMT, Germany). All samples have been coated by gold and acceleration voltage of 15 kV has been used. The diameter of was measured by image analyzer program and the mean value was reported as diameter of samples.

2.3.2 Transmission electron microscopy (TEM) Analysis

In order to study the morphology and size of CNF, TEM (model: Libra 120, Carl Zeiss, Germany) have been utilized. In this process carbon coated grid was used to deposit a drop of diluted CNF suspension. Image captured at acceleration voltage of 120 kV. The diameter of nanofibers was measured by image analyzer program and the mean value was reported as diameter of samples.

2.3.3 Fourier Transforms infrared (FTIR) spectroscopy

Changing the functional groups of samples (raw, cellulose and CNF) in each steps have been determined by FTIR spectroscopy (model: IS10 Nicolet, Thermo scientific, USA). Oven dried samples are mixed with KBr to do the test. Transparent pellet was prepared from this blend and analyzed in 400-4000 cm^{-1}.

2.3.4 X-Ray Diffraction (XRD) analysis

The crystallinity measurement of raw, cellulose and CNF was performed using X-ray Diffraction System (model: D8 Advanced Bruker, Germany). The operating voltage and current were 40 kV and 44 mA, respectively. The crystallinity (X_{CR}) was determined by the following equation:

$$X_{CR} = \frac{I_{200} - I_{AM}}{I_{200}} \times 100 \quad (1)$$

In this equation, I_{200} corresponds to crystalline and amorphous regions while I_{AM} represent amorphous region (Shi et al., 2011).

2.3.5 Thermogravimetric analysis (TGA)

Thermal decomposition temperature of raw, cellulose and CNF has been measured in nitrogen atmosphere by TGA (model: TGA/SDTA 851, Mettler Toledo, Switzerland). The temperature and heating rate was set at 25-550°C and 20°C/min, respectively.

2.3.6 Differential scanning calorimetry (DSC)

DSC (model: Perkin- Elmer DSC- 821) instrument was utilized to evaluate thermal behavior of raw, cellulose and CNF. Samples were heated under nitrogen flow from 25°C to 450°C with heating rate of 10°C/min.

2.4 Composite characterization

2.4.1 Mechanical properties

Tensile test

The tensile modulus and strength of neat epoxy composite and CNF reinforced nanobiocomposite were determined based on ASTM D 3039 and by Intron 5582 test machine. The dimensions of samples were 120mm × 15mm × 4mm.The gauge length and testing speed was set at 60mm and 5 mm/min, respectively. For each composite, five specimens were tested and the mean value represented as the final test result.

Flexural Test

Flexural test was conducted using three point bending test based on ASTM D790 and by Instron 5582 test machine with crosshead speed of 2 mm/min. The dimensions of samples were 160mm × 20mm × 4mm. For each composite, five specimens were tested and the mean value of flexural strength and modulus represented as the final test result.

Izod notched impact test

The impact test was performed in Geotech testing machine (model: GT-7045-MDL) with sample's dimension of 70mm × 15mm × 4mm and based on ASTM D 256. For each composite, five specimens were tested and the mean value of load at first deformation represented as impact strength.

2.4.2 Physical properties

Density

The density of composites was determined using ASTM D1895. For each composite, five reputations were utilized. The density of nanocomposites samples were measured using the Equation 2.

$$\text{Density}\ (\text{gcm}^{-3}) = \frac{m}{v} \qquad (2)$$

Where, m represents the mass of nanocomposites (g); v represents the volume of nanocomposites (cm^3); In order to determine mass of nanocomposites, Mettler 5000 analytical balance was applied. The volume of samples was calculated by Mitutoyo digital veneer caliper.

Water absorption

To do this test first the weight of composite samples were measured before immersing in water at ambient temperature. After one day the samples removed, gently dried with tissue to eliminate water in surface and weighted. This process was continued until getting constant weight. Water absorption percentage can be calculated according to ASTM D570 and by the following equation:

$$\text{Water absorption}(\%) = \frac{W_n - W_d}{W_d} \times 100 \qquad (3)$$

W_n and W_d are weight of composite after and before of immersion, respectively.

2.4.3 Morphological properties

Fracture surface of neat epoxy composite and nanobiocomposites were observed using SEM (model: EVO MA10, Carl-ZEISS, Germany). Samples were gold coated and the accelerating voltage set at 5 kV.

2.4.4 Thermal properties analysis

Weight loss and thermal degradation temperature of nanobiocomposites have been measured in nitrogen atmosphere by TGA (model: Perkin Elmer TGA7, USA). The temperature and heating rate was set at 25-600°C and 20°C/min, respectively.

3. Results and Discussions

3.1 Raw Fiber Analysis

3.1.1 Morphological Properties of Raw EFB Fiber

Electron microscope provides a unique tool for investigating cell wall ultrastructure. Electron microscopy observations showed that wood cell walls are composed of an intercellular layer, a primary and secondary wall. The primary cell wall is a thin layer produced by cell division and the subsequent growth of xylem mother cells while the secondary wall is a thick layer deposited inside the primary wall. It consists of an outer layer (S_1), a middle layer (S_2) and an inner layer (S_3), each with a different orientation of cellulose microfibrils (Harada & Cote, 1985).

Transmission electron microscopy (TEM) view of transverse sections of oil palm EFB fibers were showed in Figure 8. The electron microscopic observations were restricted mainly to the walls of fibers within the vascular bundles. Generally, all fibers showed great variability in size, shape and structure of the cell wall. The TEM electron micrographs have confirmed that the layered structure of EFB fiber wall contained primary (P) and secondary (S_1, S_2 and S_3) wall layers. This structure was similar to wood cell wall structure that has been proposed by Harada & Cote (1985). A typical tertiary wall is not present but warts cover the innermost layer of the cell wall.

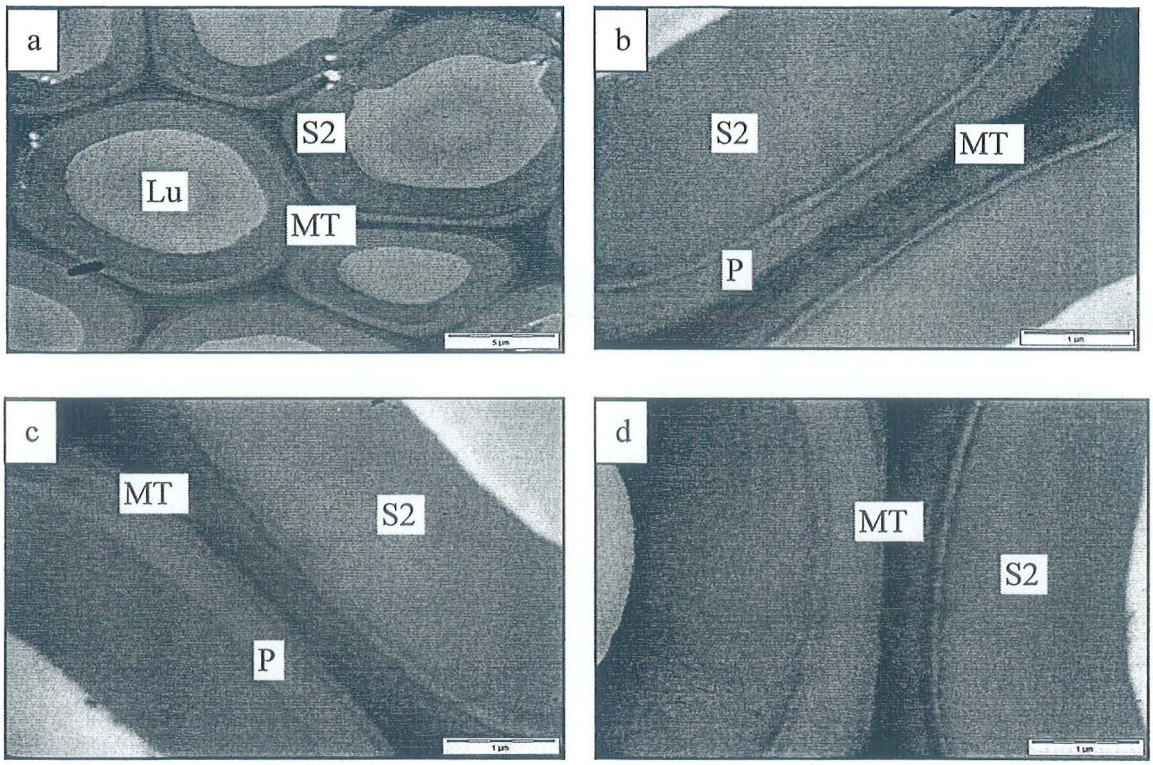

Figure 8: (a) EFB fiber cross section. Lumen Lu; MT Middle lamellae; S2 secondary wall (3400×), (b) EFB fiber cross-section showing the primary wall thicker than the walls of the S1 layer. P primary wall; MT middle lamella; S1 and S2 secondary wall (17000×), (c) EFB fiber cross-section showing S1 wall being distinguished from other wall layers on account of bright color. P primary wall; MT middle lamella; S1 and S2 secondary wall (17000×), (d) EFB fiber cross-section showing the S2 wall layer being clearly distinguished from the adjacent wall. MT middle lamella; S1 and S2 secondary wall (18 000×)

3.1.2 Fiber Anatomy and Lignin Distribution

Palms do not posses cambium and hence their "wood" is primary tissue and is not comparable in developmental terms to the wood of dicotyledons and gymnosperms. Thus, unlike the wood of dicotyledons and gymnosperms which is mostly secondary xylem, the "wood" of palm consists of primary vascular bundles imbedded in parencymatous ground tissues (Parthasarathy & Klotz, 1976). EFB fibers were hard and tough multicellular fibers with a central portion called "lacuna", (Figure 9). Sreekala (1997) reported that this porous surface morphology is useful for better mechanical interlocking with the matrix resin for composite fabrication. The cross section of the fibers was rounded to polygonal in shape. Vascular bundle of EFB fibers was a simple bundle surrounded by a sheath of thickened cell layer.

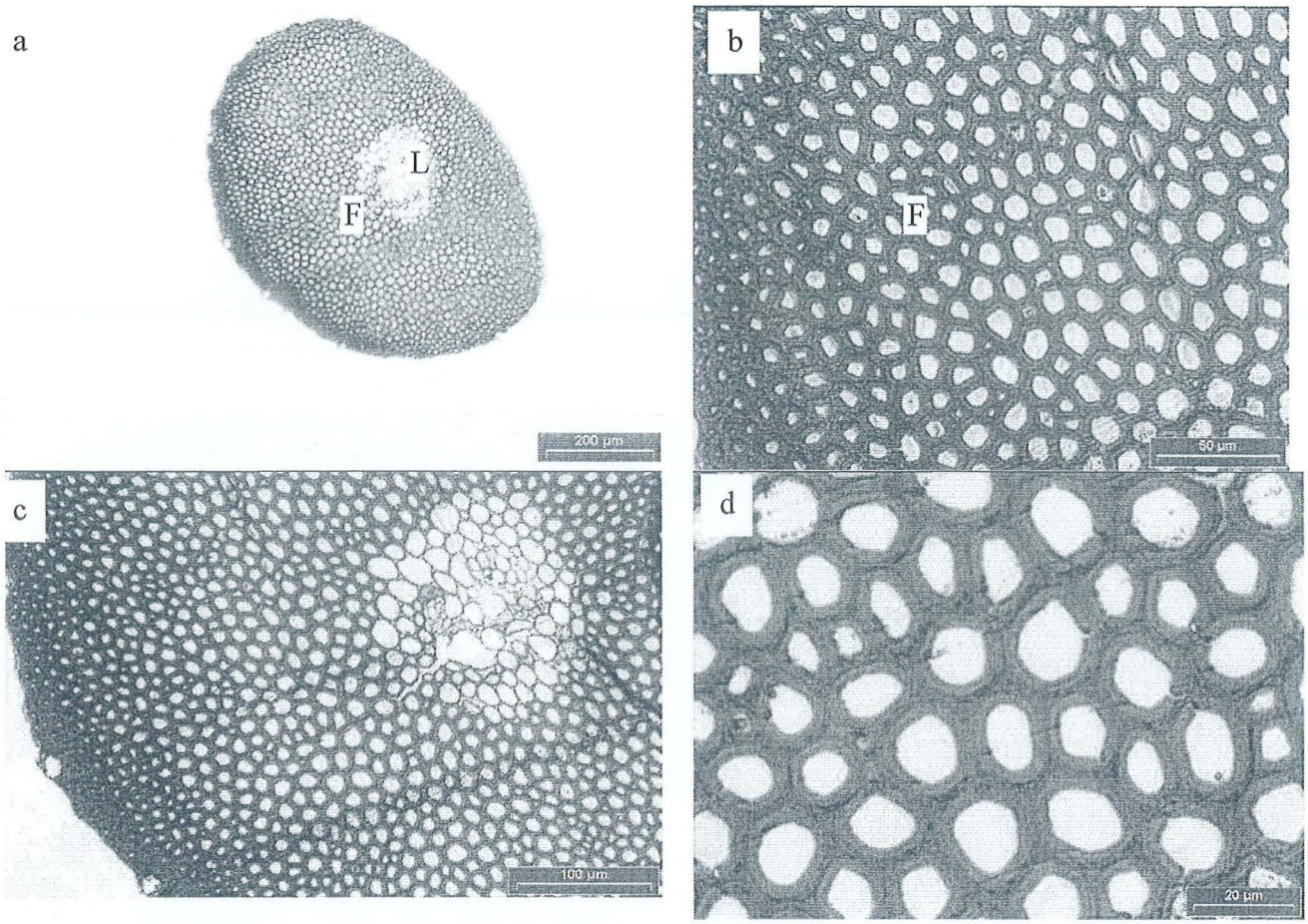

Figure 9: (a) Cross section of EFB fibers at low magnification shows vascular bundle with the void in the middle known as Lacuna (4×). L Lacuna; F Fiber, (b) Cross section of EFB fibers at high magnification show vascular bundle varies in size (20×). F Fiber, (c) Cross section of EFB fibers at low magnification show thick wall fibers at the outer vascular bundle were highly stained with dark blue (10×), (d) Cross section of EFB fibers at high magnification show fiber cell walls were positive staining with toluedine blue (40×).

3.1.3 Fiber Dimension and Derived values

Table 1 showed the length, diameter, lumen diameter, cell wall thickness and derived values of EFB fibers. According to previous study, cell length varies greatly both within and among trees. The characteristic is strongly genetically controlled. In paper technology, fiber strength, length and bonding within the web all interrelate to determine tear strength. The longer the average fiber length, the higher will be the tear resistance and folding strength of the final product in general which suitable to be used to produce paper with high tear and folding strength.

Cell dimension ratios of many types of fiber have been used to better categorize wood according to its potential utility in various products. The Runkel ratio is a microscopic extension of the plant density in that cell wall thickness and lumen width are the basic factors used in their determination (Horn, 1974). EFB fibers have low slenderness ratio, but still very good flexibility and Runkel ratio which can yield pulps with acceptable breaking length, tear and burst indices (Ververis et al., 2003).

Table 1: Length, Diameter, Lumen Diameter, Cell Wall Thickness and Derived Values of oil palm empty fruit bunch fiber

Length (mm)	0.58
Diameter (μm)	8.26
Lumen Diameter (μm)	8.89
Cell Wall Thickness :	
Primary Wall (μm)	0.37
S_1 Wall (μm)	0.08
S_2 Wall (μm)	1.55
S_3 Wall (μm)	0.034
Derived values :	
Runkel Ratio	0.464
Slenderness ratio	37.35
Flexibility coefficient	105

3.2 Mechanical Properties

3.2.1 Single Fiber Testing (Bundle)

Mechanical properties of EFB fibers were comparatively characterized and evaluated for potential application as reinforcement in polymeric composites. Linear and non-linear behaviors were observed for stress-strain curves of EFB fibers. Stress-strain curve of EFB fibers was found to include some plastic flow. Introduction of natural fibers from renewable resources for structural composites can offer acceptable properties and provides benefits to the environment by replacing synthetic fibers according to the applications. Figure 10 show the mechanical properties in single fiber testing of oil palm empty fruit bunch.

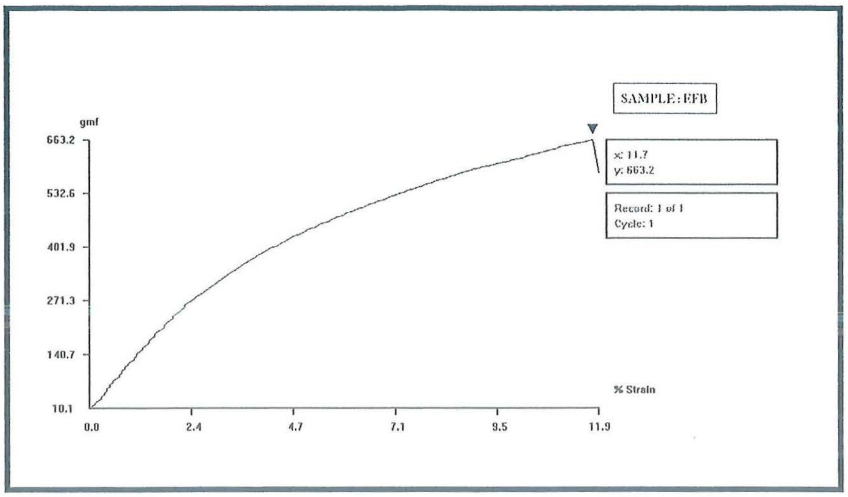

Figure 10: Mechanical properties in single fiber testing of oil palm empty fruit bunch fiber

3.2.2 X-ray Diffraction

Figure 11 and Table 2 illustrate X-ray diffractogram and crystalline percentage for OPEFB fibers. Two major diffraction peaks were observed at approximately 18° and 22° which corresponded to the (101) and (002) crystal planes, respectively. Peak intensity of 101 corresponds to amorphous area and the reading intensity of 002 lattices represents crystalline materials. These peaks could attribute to cellulose I and indicated that all the fiber was semi-crystalline.

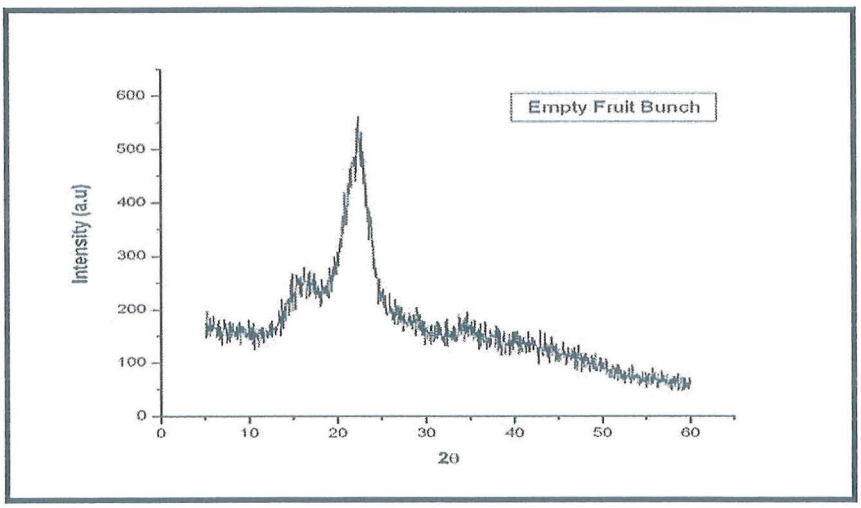

Figure 11: X-Ray diffraction graph of oil palm empty fruit bunch fiber

Table 2: Crystalline percentage of oil palm empty fruit bunch fiber

Fiber	Crystalline (%)
Empty Fruit Bunch (EFB)	58.1

3.2.3 Chemical Analysis

Table 3 shows the various chemical compositions present in EFB fiber. The data showed that in EFB fibers, amount of holocellulose is the highest (80%) while the lowest composition is ash content (3%).

Table 3: Chemical composition of oil palm empty fruit bunch fiber

	Extractive (%)	Holocellulose (%)	α-cellulose (%)	Lignin (%)	Ash (%)
EFB	3.21	80.09	50.49	17.84	3.43

3.2.4 *Forurier Transform Infrared*' (FT-IR) Spectroscopy

Fourier transform infrared (FT-IR) spectroscopy was used to detect the presence of the functional groups that exists in fibers. FT-IR spectroscopy is a powerful tool for studying the physico-chemical and conformational properties of polysaccharides. A FT-IR spectrum for the OPEFB is shown in Figure 12.

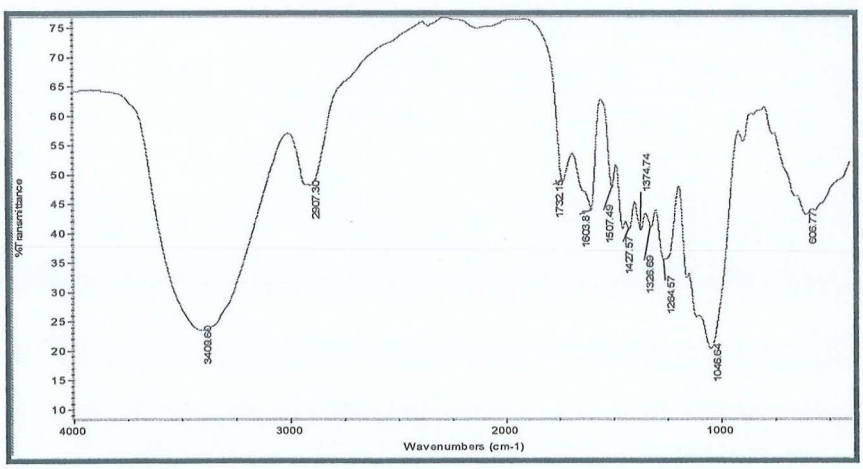

Figure 12: FT-IR spectra for the oil palm empty fruit bunch fiber

3.2.5 Thermal Properties

Thermal analysis is an important analytical method for understanding the structure-property relationship of different polymeric materials, especially fiber reinforced composites. EFB fibers is a natural lignocellulosic polymers, are subjected to thermal degradation during composite processing. Thermogravimetric (TG) and Differential Scanning Calorimetry (DSC) analysis (Figure 13) are the most widely used techniques in this area. It is useful for the thermal characterization of both inorganic and organic materials, including polymers. It provides quantitative results regarding the loss of mass of a sample as a function of increasing temperature or time.

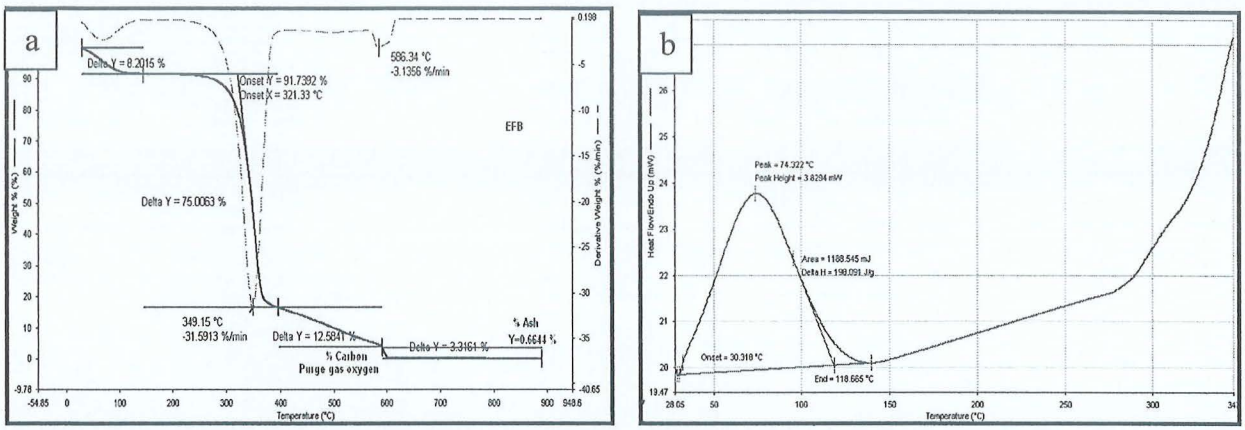

Figure 13: (a) Thermogravimetric Analysis (TGA) and (b) Differential Scanning Calorimetry (DSC) graphs of oil palm empty fruit bunch fiber

3.3 Cellulose Nanofibril Characterization

3.3.1 Morphology of EFB Raw, Cellulose and CNF Fiber

The FESEM images and diameter of raw and cellulose EFB fibers can be seen in Figure 14 (a) and (b) respectively while TEM image of cellulose nanofibrils (CNF) after passing through HPH can be seen in Figure 14 (c) and (d). The surface of raw fiber is covered by waxy materials but in contrast with the cellulose fibers which are smoother and had a smaller diameter obtained. The diameter size of EFB cellulose nanofibrils is in the range of 5-15 nm (Table 4).

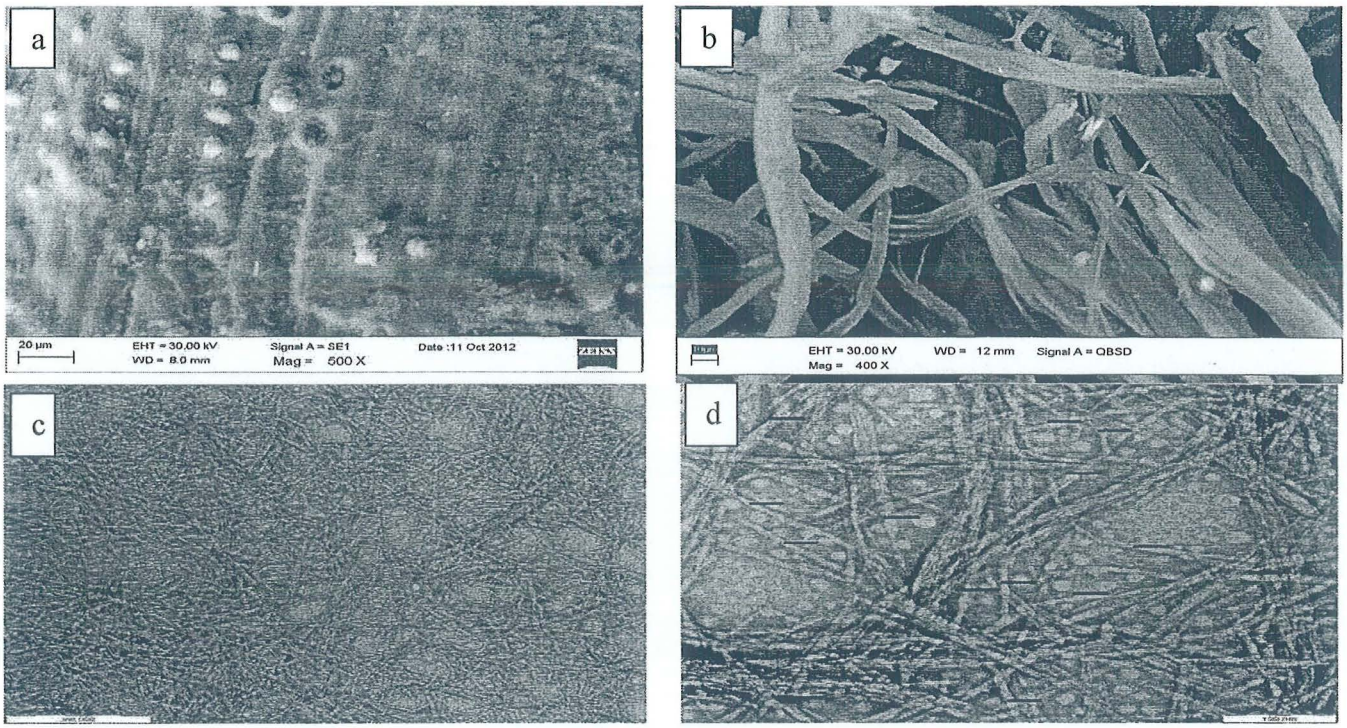

Figure 14: (a) Empty fruit bunch raw fiber structure showed the surfaces of the fiber are not smooth and tangled with lignin binder (500x), (b) Empty fruit bunch cellulose fiber structure showed a smooth and clear surface. The fibres were individualize with significant decrease in diameter (400x), (c) Empty fruit bunch cellulose nanofibrils at low magnification (12x), (d) Empty fruit bunch cellulose nanofibrils at high magnification (50x)

Table 4: Diameter size of empty fruit bunch raw, cellulose and cellulose nanofibrils

	Raw	Cellulose	CNF
Diameter	50 µm	10 µm	5 nm

3.3.2 *'Forurier Transform Infrared'* (FTIR) Spectroscopy of EFB Raw Fiber and CNF

Reduction of intensity of peaks or disappearance of any peak in FTIR analysis can give good information about changing in functional groups of our fibers after different steps. In Table 5, the disappearance of peaks 1737.18 cm^{-1}, 1508.50 cm^{-1} and 1249.35 cm^{-1} in raw fiber and CNF confirmed that lignin and hemicelluloses were removed from raw fibers during these chemical processes.

Table 5: FTIR Spectroscopy of empty fruit bunch raw fiber and cellulose nanofibrils

Peaks / Bands	Raw	CNF
	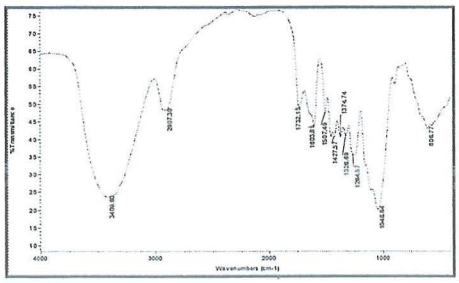	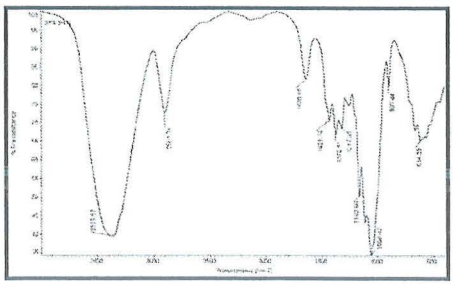
2903-2931 cm^{-1} C-H stretching Cellulose	✓	✓
1160-1189 cm^{-1} C-O-C stretching Cellulose, hemicellulose	✓	✓
1445-1602 cm^{-1} C=C stretching Lignin	✓	X
1659-1739 cm^{-1} C=O stretching Lignin, hemicellulose	✓	X
1246-1365 cm^{-1} Phenolhydroxyl stretching and C-O aromatic Lignin	✓	X

3.3.3 X-Ray Diffraction of EFB Raw Fiber, Cellulose Fiber and CNF

Table 6 and Figure 15 show the crystalline percentage and x-ray diffractograms of raw, cellulose and CNF respectively. According to the equation the crystallinity index 58%, 76% and 40% were obtained for raw, cellulose and CNF, respectively. According to results, the crystallinities of fibers increased from raw to cellulose fibers due to removal of lignin and hemicelluloses. About

CNF, a significant reduction in crystallinity index may be is due to peeling off some surface crystals during HPH.

Table 6: Crystalline percentage of empty fruit bunch raw, cellulose and cellulose nanofibrils

Fiber	Crystalline (%)
Raw	58.1
Cellulose	76.2
CNF	40.1

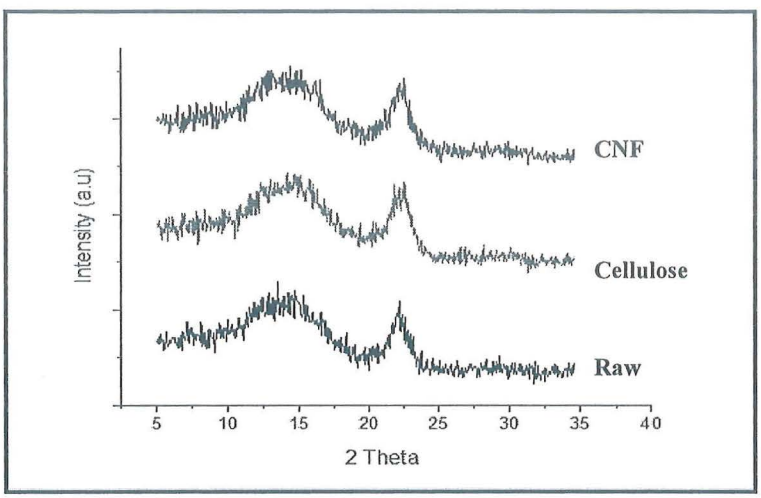

Figure 12: X-ray diffraction graph of empty fruit bunch raw, cellulose and cellulose nanofibrils

3.4 Thermal Properties

3.4.1 Thermogravimetric Analysis (TGA)

The mass loss of raw, cellulose and CNF fiber based on TGA analysis is shown in Table 7. As TGA curves illustrate the first mass loss for all fibers occurred between 30-100°C which is associated to dehydration. The residue of 20%, 10% and 7% were obtained for raw, cellulose and CNF respectively. The main decomposition was happened at 389°C, 383°C and 379°C for raw, cellulose and CNF. The reduction of thermal decomposition temperature from raw to CNF is probably because of decrease molecular weight of fibers after acid treatment which leads to decomposition at lower temperature (Kargarzadeh et al., 2012).

Table 7: TGA graph and properties of empty fruit bunch raw, cellulose and cellulose nanofibrils

	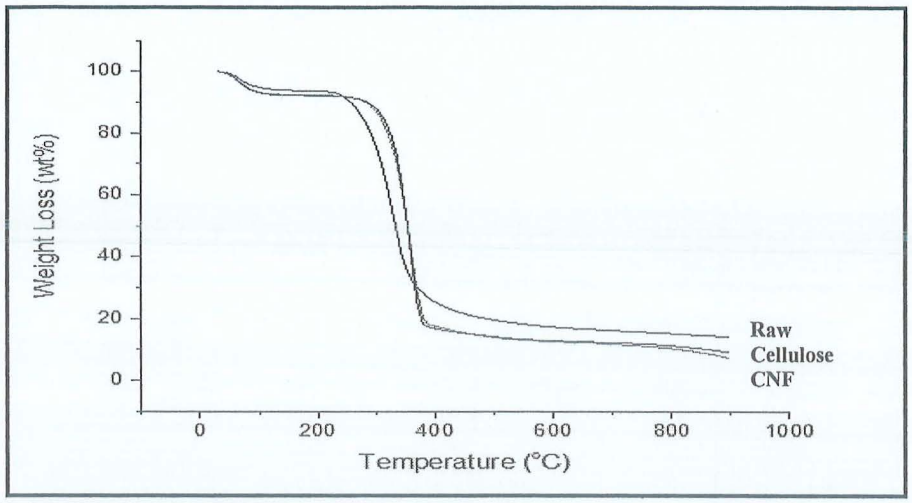
First Mass Loss (Below 100°C)	- 7% weight loss in all fibers - gradual evaporation of absorbed moisture - dehydration of fibers - released volatiles
Second Mass Loss (200 - 450°C)	- cellulose, hemicellulose and lignin decomposed
Initial Degradation Temperature (IDT),°C	Raw – 229 Cellulose – 300 CNF – 305
Final Degradation Temperature (FDT),°C	Raw – 389 Cellulose – 383 CNF - 379
After temperature 370°C - % residue	Raw – 20 Cellulose – 10 CNF – 7

3.4.2 Differential Scanning Calorimetry (DSC)

In order to evaluate the thermal behavior of materials at different steps, DSC analysis was done on raw, cellulose and CNF, displayed in Table 8. As can be observed from this figure, there is a broad endothermic peak bellow 100°C in all samples which is related to evaporation of water. The strong endothermic peak at 277°C, 348°C and 358°C for raw, cellulose and CNF was due to

cellulose degradation. Generally, increasing the decomposition temperature confirms rising of thermal stability of fibers from raw to CNF.

Table 8: DSC graph and properties of empty fruit bunch raw, cellulose and cellulose nanofibrils

	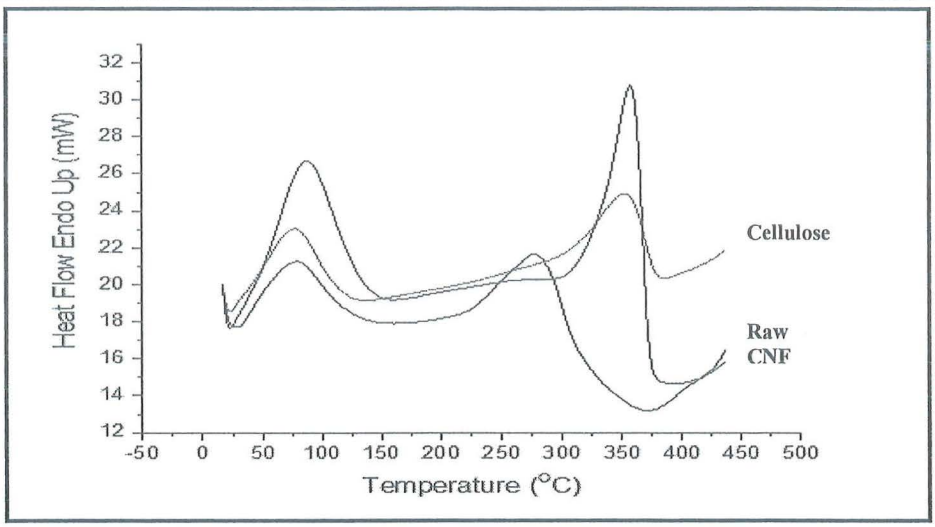
Initial Broad Endothermic (65-80°C)	Bound wáter present in all fibers
Second Broad Endotherms, °C	Raw – 277 Cellulose – 348 CNF – 358

3.5 Nanobiocomposite Characterizations

3.5.1 Fracture Surface Morphologies

The tensile fracture surface of neat epoxy (NE) composite and nanobiocomposite (N) are shown in Figure 13. As can be seen in these figures, the surface of neat epoxy is smooth and it show brittle nature of neat composite. On the other hand, the fracture surface of CNF reinforced nanobiocomposite became rougher.

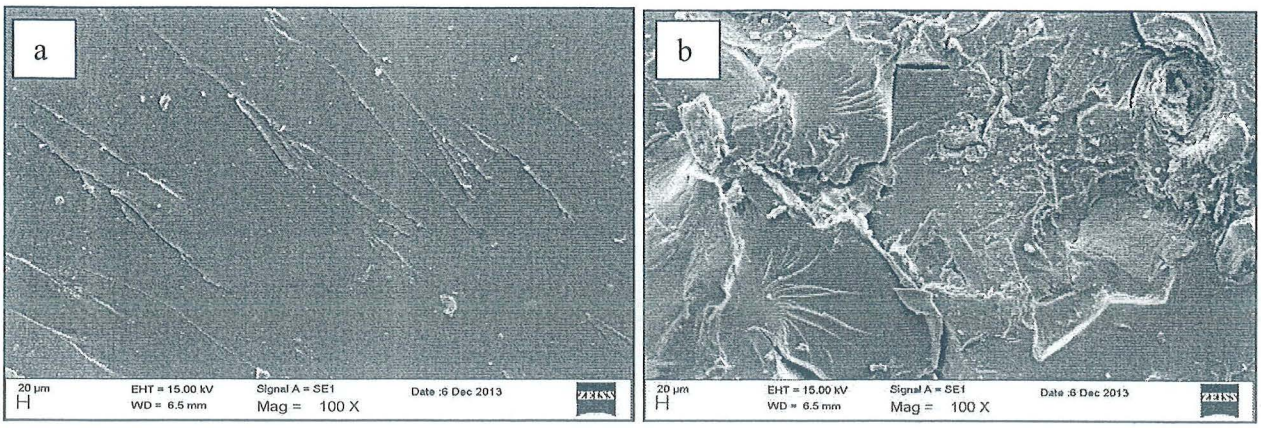

Figure 13: SEM images of tensile fracture surface of (a) neat epoxy and (b) 0.5% reinforced nanobiocomposite

3.5.2 Mechanical Properties

3.5.2.1 Tensile, Flexural and Impact Strength

Tensile, flexural and impact properties of neat epoxy composites and nanobiocomposite are tabulated in Table 9. As can be observed, properties for tensile and flexural including strength and modulus of nanobiocomposite increased with addition of 0.5% CNF loading. It might be due to high surface area of nanofibers and good interfacial bonding between nanofiller and matrix in low CNF content which prevent from quick crack propagation and help to better stress transfer. Reduction in elongation at break (from 6.9% in neat epoxy to 2.1% in 0.5% CNF reinforced nanobiocomposite) may be is due to more rigidity of CNF compare to brittle nature of epoxy, which cause to diminish the amount of existing epoxy for elongation and therefore reduce elongation at break (Abdul Khalil et al., 2013). The impact strength of 8.9 and 7.1 (J/m^1) was obtained for neat epoxy and 0.5% CNF reinforced nanobiocomposite, respectively.

Table 9: Tensile, flexural and impact strength of neat epoxy (NE) and nanobiocomposite (N)

	Tensile			Flexural		Impact (Jm^{-1})
	Strength (MPa)	Modulus (GPa)	Elongation (%)	Strength (MPa)	Modulus (GPa)	
NE	23.9	0.7983	6.91	24.3	1.1129	8.93
N	27.4	1.0649	2.08	28.2	1.1976	7.05

3.5.2.2 Density and Water Absorption

Table 10 shows the density of neat epoxy composite and nanobiocomposite. The density of nanobiocomposites after addition of CNF increased from 1.15 to 1.18 gr/cm^3 is because of incorporating high density cellulose nanofiber with low density epoxy resin. Water absorption behavior of nanobiocomposites is shown in Figure 14. It can be seen that mixing of CNF increase water absorption of nanobiocomposite. Higher water absorption in 0.5% CNF nanobiocomposite probably is due to higher amount of CNF which is hydrophilic in nature and can absorb more water.

Table 10: Density of neat epoxy composites and nanobiocomposite

Fiber	Density (gr/cm^3)
Neat epoxy	1.15
0.5 % CNF nanobiocomposite	1.18

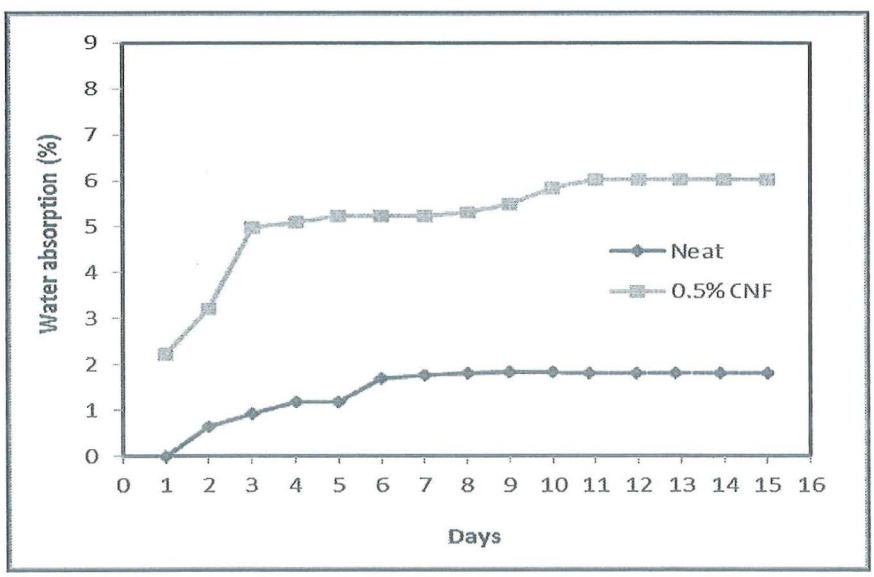

Figure 14: Water absorption behaviour of neat epoxy composite and nanobiocomposite

3.5.3 Thermal Properties

3.5.3.1 Thermogravimetric Analysis (TGA)

TGA analysis of neat epoxy composites and nanobiocomposites are exhibited in Figure 15. All samples exhibited initial weight loss below 100°C because of removing moisture. Main degradation temperature for neat and 0.5% CNF were 359°C and 447°C, respectively. Incorporation of CNF at low concentration had led to increasing thermal stability of nanobiocomposites may be due to high cellulose content of nanofiller. It is believe that maybe by increasing the percentage of CNF thermal stability of nanobiocomposite become higher than neat epoxy. The amount of residue is shown in Table 11. By adding the CNF the char residues decreased gradually maybe because of purity of the nanofiller.

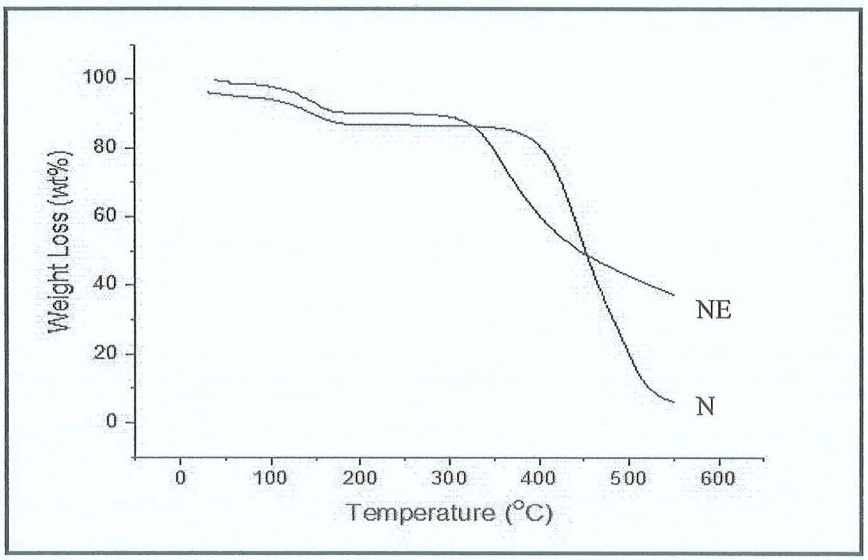

Figure 15: TGA curves of neat epoxy (NE) and 0.5% CNF reinforced nanobiocomposite (N)

Table 11: TGA properties of neat epoxy (NE) and nanobiocomposite (N)

	TGA			
	IDT (°C)	FDT (°C)	DTG (°C)	Residue (%)
NE	330	450	359	34.8
N	425	525	447	5.3

4. Conclusion

In this present research project, nanofibrillated cellulose fibers were successfully isolated from oil palm empty fruits bunch using combination of sulphuric acid hydrolysis and high pressure homogenization processes. Results showed that acid concentration and acid to fiber ratio play effective role in the fibrillate formation of cellulosic fibers. Analyses of the SEM images revealed that acid hydrolysis treatment did not affect the morphological structure of the treated fibres, but it exhibits in a smaller particle dimension. Transmission electron micrographs analysis revealed that the nanofibrillation of the OPEFB cellulose fiber diameters within the range of 5 to 10 nm. FT-IR analysis indicated that the acid hydrolysis did not influence the chemical structure of the treated fibre and effectively remove lignin and hemicellulose from the raw cellulosic fiber. X-RD analysis showed that percentage crystallinity of nanofibrillated cellulose notably influenced by pressure of HPH. However, the TGA analyses exposed that the isolated NFC had the trustworthy maximal thermal durability. Based on the results, it was evident that the isolation of NFC fibers using combination of sulphuric acid hydrolysis and high pressure homogenization processes has the potentiality to be quality reinforcing agent for composite materials, because of prospective thermal stability along with minimal particle size formation. Thus, the combination of sulphuric acid hydrolysis and high pressure homogenization processes could be utilized as a novel chemo-mechanical process for the isolation CNF with good mechanical and thermal properties, confirm the potentiality of the nanobiocomposite for various engineering applications.

References

Abdul Khalil, H., A. Yusra, et al. (2010). "Cell wall ultrastructure, anatomy, lignin distribution, and chemical composition of Malaysian cultivated kenaf fiber." Industrial Crops and Products 31(1): 113-121.

Alemdar, A. and M. Sain (2008). "Isolation and characterization of nanofibers from agricultural residues–Wheat straw and soy hulls." Bioresource technology 99(6): 1664-1671.

Ang, L. S., C. P. Leh, et al. (2010). "Effects of alkaline pre-impregnation and pulping on Malaysia cultivated kenaf (Hibiscus cannabinus)." BioResources 5(3): 1446-1462.

Ashori, A., W. D. Raverty, et al. (2006). "Effect of totally chlorine free and elemental chlorine free sequences on whole stem kenaf (Hibiscus cannabinus) pulp characteristics." Polymer-Plastics Technology and Engineering 45(2): 205-211.

Bhatnagar, A. and M. Sain (2005). "Processing of cellulose nanofiber-reinforced composites." Journal of Reinforced Plastics and Composites 24(12): 1259-1268.
Bledzki, A. and J. Gassan (1999). "Composites reinforced with cellulose based fibres." Progress in polymer science 24(2): 221-274.
Chan, H. C., C. H. Chia, et al. (2012). "Production and Characterisation of Cellulose and Nano-Crystalline Cellulose from Kenaf Core Wood." BioResources 8(1).
Henriksson, M., L. A. Berglund, et al. (2008). "Cellulose nanopaper structures of high toughness." Biomacromolecules 9(6): 1579-1585.
Jonoobi, M., K. O. Niska, et al. (2009). "Chemical composition, crystallinity, and thermal degradation of bleached and unbleached kenaf bast (Hibiscus cannabinus) pulp and nanofibers." BioResources 4(2): 626-639.
Jonoobi, M., A. P. Mathew, et al. (2012). "A comparison of modified and unmodified cellulose nanofiber reinforced polylactic acid (PLA) prepared by twin screw extrusion." Journal of Polymers and the Environment 20(4): 991-997.
Kamel, S. (2007). "Nanotechnology and its applications in lignocellulosic composites, a mini review." Express Polym Lett 1(9): 546-575.
Kargarzadeh, H., I. Ahmad, et al. (2012). "Effects of hydrolysis conditions on the morphology, crystallinity, and thermal stability of cellulose nanocrystals extracted from kenaf bast fibers." Cellulose 19(3): 855-866.
Khalil, H. A. and N. L. Suraya (2011). "Anhydride modification of cultivated kenaf bast fibers: morphological, spectroscopic and thermal studies." BioResources 6(2): 1121-1135.
Li, J., X. Wei, et al. (2012). "Homogeneous isolation of nanocellulose from sugarcane bagasse by high pressure homogenization." Carbohydrate polymers.
López-Rubio, A., J. Lagaron, et al. (2007). "Enhanced film forming and film properties of amylopectin using micro-fibrillated cellulose." Carbohydrate polymers 68(4): 718-727.
Lu, J., T. Wang, et al. (2008). "Preparation and properties of microfibrillated cellulose polyvinyl alcohol composite materials." Composites Part A: Applied Science and Manufacturing 39(5): 738-746.
Masoodi, R., R. El-Hajjar, et al. (2012). "Mechanical characterization of cellulose nanofiber and bio-based epoxy composite." Materials & Design 36: 570-576.
Shi, J., S. Q. Shi, et al. (2011). "A chemical process for preparing cellulosic fibers hierarchically from kenaf bast fibers." BioResources 6(1): 879-890.
Siqueira, G., J. Bras, et al. (2010). "Cellulosic bionanocomposites: a review of preparation, properties and applications." Polymers 2(4): 728-765.
Webber III, C. L., H. L. Bhardwaj, et al. (2002). "Kenaf production: fiber, feed, and seed." Trends in new crops and new uses. ASHS Press, Alexandria.

Cellulosic Nanocomposites from Natural Fibers for Medical Applications: A Review

25

H. P. S. Abdul Khalil, A. H. Bhat, A. Abu Bakar, M. T. Paridah, I. S. M. Zaidul, and M. Jawaid

Contents

H.P.S. Abdul Khalil (✉)
School of Industrial Technology, Universiti Sains Malaysia, Penang, Malaysia
e-mail: akhalilhps@gmail.com

A.H. Bhat
Fundamental and Applied Sciences, Universiti Teknologi Petronas, Perak, Malaysia
e-mail: bhataamir@gmail.com

A. Abu Bakar
Materials and Mineral Resources Engineering, Universiti Sains Malaysia, Penang, Malaysia
e-mail: azhar@eng.usm.my

M.T. Paridah
Institute of Tropical Forestry and Forest Products, Universiti Putra Malaysia, Serdang, Selangor, Malaysia
e-mail: parida.introp@gmail.com

I.S.M. Zaidul
Faculty of Pharmacy, International Islamic University Malaysia, Kuala Lumpur, Malaysia
e-mail: zaidul@iium.edu

M. Jawaid
Department of Biocomposite Technology, Institute of Tropical Forestry and Forest Products, Universiti Putra Malaysia, Serdang, Selangor, Malaysia
e-mail: akhalilhps@gmail.com

J.K. Pandey et al. (eds.), *Handbook of Polymernanocomposites. Processing, Performance and Application – Volume C: Polymer Nano-composites of Cellulose Nano-particle*,
DOI 10.1007/978-3-642-45232-1_72, © Springer-Verlag Berlin Heidelberg 2014

878 interaction, to be a promissory biomaterial and may be suitable for cell adhesion/
879 attachment, suggesting that these scaffolds can be used for wound dressing or
880 tissue-engineering scaffolds [161].

8 Conclusions

881 The potential applicability of cellulose-based biocomposites and nanocomposites
882 are widely extended. Due to a great number of properties, applications of
883 nanocellulose-based materials are mainly considered to be in a wide range of
884 biomaterial applications such as medical products, pharmacy, cosmetics, dental,
885 and veterinary applications are also being considered. The mechanical properties
886 such as high strength and stiffness, the surface reactivity (with numerous hydroxyl
887 groups), and the specific organization as well as the small dimensions of
888 nanocellulose may well impart useful properties to nanocomposite materials
889 reinforced with these fibers.

890 The aim of this article was to demonstrate the current state of research and
891 development in the field of nanocellulose – a biofabricated sustainable type of
892 polymer material. The extraordinary supramolecular nanofiber network structure
893 and the resulting valuable properties have led to real opportunities and extensive
894 activity in the field of biomedical applications. The intention of this work is to
895 broaden the knowledge in this subject area and to stimulate the practical application
896 of nanocellulose. In the biomedical field, bacterial nanocellulose implants have
897 opened up new uses for bioartificial medical devices.

898 **Acknowledgement** The authors would like to express gratitude for extending their support in the
899 form of Research University (RU) grant (1001/PTEKIND/814133)

900 References

901 1. Nakagaito AN, Yano H (2005) Novel high-strength biocomposites based on microfibrillated
902 cellulose having nano-order-unit web-like network structure. Appl. Phys. A: Mater. Sci.
903 Process 80:155–159
904 2. Nakagaito AN, Yano H (2004) The effect of morphological changes from pulp fibre towards
905 nano- scale fibrillated cellulose on the mechanical properties of high-strength plant fibre
906 based composites. Appl Phys A: Mater Sci Process 78:547
907 3. Bledzki AK, Reihmane S, Gassan J (1996) Properties and modification methods for vegeta-
908 ble fibers for natural fiber composites. J Appl Polym Sci 5:1329
909 4. Hornsby PR, Hinrichsen E, Tarverdi K (1997) Preparation and properties of polypropylene
910 composites reinforced with wheat and flax straw fibers. J Mater Sci 32:1009
911 5. Oksman K, Wallstrom L, Berglund LA, Filho RDT (2002) Morphology and mechanical
912 properties of unidirectional sisal-epoxy composites. J Appl Polym Sci 84:2358
913 6. Nabi Saheb D, Jog JP (1999) Natural fiber polymer composites: a review. Adv Polym
914 Technol 18:351
915 7. Georgopoulos ST, Tarantili PA, Avgerinos E, Andreopoulos AG, Koukios EG (2005)
916 Thermoplastic polymers reinforced with fibrous agricultural residue. Polym Degrad Stab
917 90:303

Termite Resistance Study of Oil Palm Trunk Lumber (OPTL) Impregnated with Oil Palm Shell Meal and Phenol-Formaldehyde Resin

Rudi Dungani,[a,b] Md Nazrul Islam,[a,c] H.P.S. Abdul Khalil,[a,d,*] Sri Hartati,[e] C. K. Abdullah,[a] Mustika Dewi,[b] and A. Hadiyane [b]

A phenol-formaldehyde (PF) resin treatment of OPTL with various concentrations of finely ground palm shell, together abbreviated PF-FGPS, has been used to improve termite resistance. Termite resistance was evaluated in two ways, in a laboratory test and in a field test that lasted 3 months. A feeding arena sample was prepared for the first experiment so that the responses of the subterranean termite (*Coptotermes curvignathus* (Holmgren)) and the drywood termite (*Cryptotermes cynocephalus* (Light)) to the laboratory test could be observed for 4 weeks and 12 weeks, respectively. In general, the PF-FGPS led to greater termite resistance than did the control (dried OPTL and rubberwood), and the resistance of the samples to the subterranean termite *C. curvignathus* was classified as moderate when the samples were treated with OPS meal. Meanwhile, the resistance of the samples to the drywood termite *C. cynocephalus* was classified as moderate when samples were treated with OPS meal concentrations of 0, 1, and 3%. The samples treated with 5% OPS meal were classified as resistant. In the field test, samples impregnated with OPS meal at levels of 3%, 5%, and 10% were classified as resistant, while those impregnated with OPS meal at levels of 0 and 1% were classified as moderately resistant to attack by the subterranean termite.

Keywords: Impregnation; Finely ground biomass; Termite; Termite resistance; Oil palm trunk; Oil palm shell

*Contact information: a: School of Industrial Technology, Universiti Sains Malaysia, 11800, Penang, Malaysia; b: School of Life Sciences and Technology, Institut Teknologi Bandung, Gedung Labtex XI, Jalan Ganesha 10, Bandung 40132, West Java-Indonesia; c: School of Life Science, Khulna University, Khulna – 9208, Bangladesh; d: Department of Biocomposite Technology, Institute of Tropical Forestry and Forest Products (INTROP), Universiti Putra Malaysia, 43400 UPM Serdang, Selangor, Malaysia; e: Department of Plant Protection, Faculty of Agriculture, Padjadjaran University, Bandung, West Java Indonesia; *Corresponding author: akhalilhps@gmail.com, akhalil@usm.my*

INTRODUCTION

The increasing world population has led to an increase in demand for wood material for construction purposes as well as for furniture. One way to overcome the shortage in wood supply is to use non-woods such as oil palm trunks (OPT). Oil palm trunk lumber (OPTL) is a very familiar material that has been used for centuries in low-cost and medium- to low-performance markets. As the economic life span of the oil palm tree is 25 to 30 years (Abdul Khalil *et al.* 2010), it is estimated that more than 70,000 ha will have to be replanted every year, requiring the felling of about 9 million palms in Malaysia alone (Mokhtar *et al.* 2008). Many researchers (Abdullah *et al.* 2012; Abdul Khalil *et al.* 2012, 2010; Jawaid *et al.* 2011; Hayawin *et al.* 2011; Bhat and Abdul Khalil

Figure 5 shows the drywood termite attack on PF-FGPS-impregnated OPTL. The drywood termites showed patterns of attack similar to those of subterranean termites. However, the drywood termite attack was less severe than the subterranean termite attack under the same treatment conditions. The drywood termites tended to cut wood across the grain by destroying both the softer springwood and the harder summerwood. They made small holes on the wood surface wherever they infested. The details of the mechanism of termite attack were described by Furukawa and Kobayashi (2006). They mentioned that the attack begins with the earlywood tracheids, which are easily bitten away and broken into a small piece by the mandible; accordingly, numerous V-shaped bite marks were left in the degraded earlywood following the attack.

CONCLUSIONS

1. Impregnation of phenol-formaldehyde resin that had been mixed with finely ground oil palm shell meal (PF-FGPS) into the oil palm trunk lumber (OPTL) improved the resistance against subterranean and drywood termite attacks by filling the cell lumens and increasing the density.
2. In laboratory conditions, the treated OPTL was categorized as moderately resistant against subterranean termites for any percentage of PF-FGPS impregnation. It was also moderately resistant against subterranean termites after a 12-week field test for any percentage of PF-FGPS impregnation except for 5%, which was categorized as resistant under the same field conditions.
3. For the drywood termite test, PF-FGPS impregnations equal to or above 3% were categorized as resistant, while the remaining impregnations were categorized as moderately resistant.
4. The advanced materials applications of finely ground meal from OPS would reduce the present environmental problems coming from this biomass, and would ensure the sustainable use of this renewable biomass resource for the future.

ACKNOWLEDGEMENTS

The author would like to thank Universiti Sains Malaysia (USM), Penang, Malaysia, for providing Research Grant no. 1001/PTEKIND/814133 for this study. The author is also thankful to Prof. Pingkan Aditiawati, School of Life Sciences and Technology, Institut Teknologi Bandung, West Java-Indonesia and Prof. Y. S. Hadi, Department of Forest Product, Faculty of Forestry, Bogor Agricultural University, West Java, Indonesia, for providing the necessary facilities for preparing the part of the research during the sabbatical leave for the period of December 1, 2011 to August 31, 2012.

CHARACTERIZATION OF VARIOUS ORGANIC WASTE NANOFILLERS OBTAINED FROM OIL PALM ASH

H. P. S. Abdul Khalil,*[a] Rus Mahayuni A. R.,[a] Irshad-ul-Haq Bhat,[b] Rudi D.,[a,c] M. Z. Almulali,[d] and C. K. Abdullah [a]

The byproducts of palm oil production (nut shells, fibers, and EFB) were combusted to obtain organic waste nanofillers. The prepared nano-filler was characterized by different techniques, *viz.* XRD for degree of crystallinity, particle size, morphology, and spectroscopic methods. The average diameter found was between 93.39 and 192.20 nm, and the width was between 18.17 and 43.45 nm. The SEM images revealed various morphological arrangements of particles. XRD studies exhibited crystalline nature of both the raw and ground nanofillers. The elemental analysis of nanofillers was carried out by EDX, and FT-IR was used to assign the degree of stretching of various functional groups. In addition to C, N, and O, elemental analysis revealed the presence of Al, Mg, Si, P, K, Ca, Fe, S, Ti, and Mn.

Keywords: Oil palm ash; Nanofillers; SEM; XRD; FT-IR

*Contact information: a: School of Industrial Technology, Universiti Sains Malaysia, Penang, 11800, Malaysia; b: Faculty of Earth Sciences, Universiti Malaysia Kelantan, Campus Jeli, 17600, Kelantan c:School of Life Sciences and Technology, Institute of Technology Bandung, Winaya Mukti 01 Jatinangor Sumedang 45363 West Java Indonesia; d: Building Technology, School of Housing Building and Planning Universiti Sains Malaysia, Penang, 11800, Malaysia; * Corresponding author: akhalilhps@gmail.com*

INTRODUCTION

The environmental concerns of burning and disposing the residues of combustible substances have grown in recent years (Lee *et al.* 2005). The ash is one of the main concerns, and substantial amounts are obtained by burning of paper, rubbish, and coal (Lee *et al.* 2005). In addition, improper handling of agricultural biowaste also leads to environmental and health problems. Waste disposal from palm oil mills in Malaysia is one of the main environmental challenges for industries after meeting the demand for oil at domestic and global levels (MPOB 2008). Malaysia alone produces millions of tons of oil palm biomass *viz.* oil palm trunks, oil palm fronds, empty fruit bunches, and therefore, the disposal of such biomass poses a great threat to the ecosystem (Ismail and Shaari 2009). Researchers have utilized the biomass obtained from this source in a sustainable economic way, for the automotive industries, paper technology, composite fabrications, and activated carbon (Abdul Khalil *et al.* 2011). The conversion of biowaste from palm oil to palm oil ash (OPA) is an alternative method to utilize this biowaste in a socio-economic way. Palm oil ash is composed of silicates and aluminates, in addition to different metal oxides and hence can be exploited in various applications *viz.* as a cement replacement, as a metal adsorbent due to its varied degree of surface area, and further processing. For instance, grinding and ball milling can generate nanoparticles, which can be explored as nanofillers for composite fabrications (Tay and Show 1996; Chu and Hashim 2002; Abdul Khalil *et al.* 2011). Nanotechnological aspects of this biowaste will

to deformation which occurred in O-H vibrations bonded to silicon atoms. The band at 1050 cm^{-1} can be also implied to structural vibration of Si-O bond of SiO_2 (Hamelmann *et al.* 2005).

CONCLUSIONS

1. This study analyzed the preparation and characterizations of oil palm ash derived at different particulate stages. The results indicate that various amounts of silica and carbon were present in the raw and ground OPA.
3. The particle size was found to be strongly dependent on the particulate stage. The morphology of particles was found to be like crushed particles.
4. In the FT-IR spectra, in addition to silicon-oxygen vibrations, silanols were also observed.
5. The produced nanomaterials from OPA may be a suitable candidate to be used as nanofiller to reinforced composites.

ACKNOWLEDGEMENT

The author would like to thank Universiti Sains Malaysia (USM), Penang, Malaysia, for providing Research Grant no. 1001/PTEKIND/814133 for this study. The author would also like to highly acknowledge and pay gratitude to the School of Life Sciences and Technology, Institute of Technology, Bandung, Winaya Mukti 01 Jatinangor Sumedang 45363 West Java, Indonesia, for providing technical support and facilities during his short visit as a visiting professor.

REFERENCES CITED

Abdul Khalil, H. P. S., Fizree, H. M., Jawaid, M., and Alattas, O. S. (2011). "Preparation and characterization of nanostructured materials from oil palm ash: A bioagricultural waste from oil palm mill," *BioResources* 6(4), 4537-4546.

Cao, G. (2004). *Nanostructures & Nanomaterials: Synthesis, Properties &. Applications*, Imperial College Press, London.

Chu, K. H., and Hashim, M. A. (2002). "Adsorption and desorption characteristics of zinc on ash particles derived from oil palm waste," *J. Chemical Technol. Biotech.* 77(6), 685-693.

Foo, K. Y., and Hameed, B. H. (2009). "Value-added utilization of oil palm ash: A superior recycling of the industrial agricultural waste," *J. Hazard. Mater.* 172, 523-531.

Hamelmann, F., Heinzmann, U., Szekeres, A., Kirov, N., and Nikolova, T. (2005). "Deposition of silicon oxide thin films in TEOS with addition of oxygen to the plasma ambient : IR spectra analysis," *J. Optoelectronics Advanced Materials* 7(1), 389-392.

Carbohydrate Polymers 87 (2012) 963–979

Contents lists available at SciVerse ScienceDirect

Carbohydrate Polymers

journal homepage: www.elsevier.com/locate/carbpol

Review

Green composites from sustainable cellulose nanofibrils: A review

H.P.S. Abdul Khalil*, A.H. Bhat, A.F. Ireana Yusra

School of Industrial Technology, Universiti Sains Malaysia, 11800 Penang, Malaysia

ARTICLE INFO

Article history:
Received 20 July 2011
Received in revised form 23 August 2011
Accepted 24 August 2011
Available online 31 August 2011

Keywords:
Cellulose
Green composites
Cellulose nanocomposites
Cellulose nanofibrils

ABSTRACT

Green composites are materials having ecofriendly attributes that are technically and economically feasible while minimizing the generation of pollution. In this context it refers to the combination of fully degradable fibers mostly cellulosic materials and natural resins to develop green composite materials. In the past decade, overdependence on petroleum products (synthetic polymers, resins, etc.) has consistently increased and on account of this, the researchers are now focusing more on green materials specially cellulosics. Cellulosic fibers in micro and nano scale are attractive to replace man-made fibers as reinforcement to make environmentally friendly green products. In this study, we will discuss the processing, extraction, properties, chronological events and applications of cellulose and cellulosic-based nanocomposite materials. Cellulosic nanocomposites are currently considered one of the most promising areas of scientific and technological development in the field of plant products. The aim of this review is to demonstrate the current state of development in the field of cellulose nanofibril based green composites research and application through examples.

Contents

* Corresponding author. Tel.: +60 4 6532200; fax: +60 4 657367.
E-mail address: akhalilhps@gmail.com (H.P.S. Abdul Khalil).

0144-8617/$ – see front matter © 2011 Elsevier Ltd. All rights reserved.
doi:10.1016/j.carbpol.2011.08.078

Table 5
Chronological order of events in the exploration of cellulose and its related applications.

Year	Progress	References
1832	Synthesis of 'Cellulose nitrate'	Braconnot, H. (1833). Ann, 1, 242, 245
1839	Payen isolates cellulose as the principal constituent of wood	Zugenmaier (2008)
1845	Invention of Cellulose esters	Schonbein, C. F. (1847). Philos. Mag., 31, 7
1983	Isolated microfibrillated cellulose by mechanical homogenization from hardwood	Herrick et al. (1983)
1998	Developed solidified liquid crystals for optical applications like in security paper	Revol, J. F., Godbout, L., & Gray, D. (1998). PPR 1331 report
2004	Prepared cellulose whiskers reinforced nanocomposites from an organic medium suspension	Azizi Samir et al. (2004)
2004	Studied cellulose microfibril-based nanocomposites for semistructural applications	Nakagaito and Yano (2004)
2004	Reinforcing agents for low-thickness polymer electrolytes for lithium batteries application	My Ahmed Said Azizi Samir, Fannie Alloin, Wladimir Gorecki, Jean-Yves Sanchez, & Alain Dufresne. (2004). J. Phys. Chem. B 108, 10845–10852
2005	Optically transparent cellulose nanocomposites	Yano, H., Sugiyama, J., Nakagaito, A. N., Nogi, M., Matsuura, T., Hikita, M., & Handa, K. (2005). Adv Mater 17:153
2006	Sisal cellulose whiskers reinforced polyvinyl acetate nanocomposites	Nancy Lis Garcia de Rodriguez, Wim Thielemans, & Alain Dufresne. (2006). Cellulose 13, 261–270
2007	Biofoams based on amylopectin-rich potato starch and cellulose nanofibres from wood pulp	Svagan, A. J., Samir, M., & Berglund, L. A. (2007). Biomacromolecules 8, 2556
2008	Biocomposites of cellulose reinforced starch: improvement of properties by photo-induced cross linking	Pratheep Kumar, A., & Raj Pal Singh. (2008). Bioresource Technology 99, 8803–8809
2008	Robust aerogels were prepared by freeze drying of cellulose nanofibre water suspensions	Paakko, M., Vapaavuori, J., Silvennoinen, R., Kosonen, H., Ankerfors, M., Lindstrom, T., Berglund, L. A., & Ikkala, O. (2008). Soft Matter 4, 2492
2008	Nanopaper from cellulose nanofibril suspensions	Henriksson, M., Berglund, L. A., Isaksson, P., Lindstrom, T., & Nishino, T. (2008). Biomacromolecules 9, 1579
2008	Reinforcing adhesives using cellulose nanofibres	Gardner, D. J., Oporto, G. S., Mills, Ryan, Samir, My Ahmed Said Âziz. (2008). 22 (5/6), 545–567(23)
2009	Cellulose microfibrils from banana rachis: effect of alkaline treatments on structural and morphological features	Zuluaga et al. (2009)
2010	Cellulose nanowhiskers from coconut husk fibers: effect of preparation conditions on their thermal and morphological behavior	Rosa et al. (2010)
2010	Isolation of nanocellulose from pineapple leaf fibers by steam explosion	Bibin Mathew Cherian, Alcides Lopes Leao, Sivoney Ferreira de Souza, Thomas, S., Pothan, L. A. & Kottaisamy, M. (2010). Carbohydrate Polymers, 81(3), 720–725

is more hydrophilic than cellulose, in moist conditions it absorbs most of the water and is then plasticized. The cellulosic network is surrounded by a soft phase and the interactions between the filler and the matrix are strongly reduced.

Besides improving mechanical properties of starch, addition of MFC to the matrix resulted in a decrease of both water uptake at equilibrium and the water diffusion coefficient. A different approach to achieve starch-nanocellulose composites has been presented by Grande et al. (2008). In their study, starch was added to the culture medium of cellulose-producing bacteria (Acetobacter sp.) in order to introduce the granules into the forming network of cellulose. The application of such a bottom-up technique allowed the preservation of the natural ordered structure of cellulose nanofibers. Fig. 13 shows SEM picture of starch cellulose nanocomposites with 10% cellulose nanofibrils. From the image, it is clear that the nanofibers are well dispersed and covered by the matrix. Fiber bundles can be observed embedded in the polymer matrix.

The BC-starch mats were hot pressed to obtain nanocomposite sheets. Atomic force microscopy and environmental scanning electron microscopy (ESEM) revealed that starch acted as a matrix which filled the voids in the BC network. The gelatinized starch formed a homogenous layer on BC fibers and a typical brittle fracture surface of the composites was observed. Using MFC, a molded product with a bending strength of 250 MPa was obtained by Yano and Nakahara (2004) without the use of binders. When 2 wt% oxidized tapioca starch was added, the yield strain doubled and the bending strength reached 310 MPa.

Recently, nanocomposites from wheat straw nanofibers and thermoplastic starch from modified potato starch was prepared by the solution casting method (Alemdar & Sain, 2008). Thermal and mechanical performance of the composites was compared with

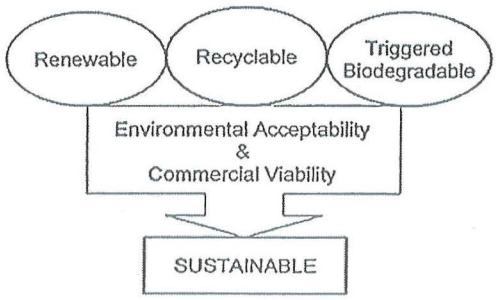

Fig. 14. Concept of "sustainable" bio-based product.

the pure thermoplastic starch using thermogravimetric analysis (TGA), dynamic mechanical analysis (DMA) and tensile testing. The tensile strength and modulus were significantly enhanced in the nanocomposite films, which could be explained by the uniform dispersion of nanofibers in the polymer matrix. The modulus of the TPS increased from 111 to 271 MPa with maximum (10 wt%) nanofiber filling. In addition, the glass transition (Tg) of the nanocomposites was shifted to higher temperatures with respect to the pure TPS. Mondragón et al. (2008) applied glyceryl monostearate (GMS) as surfactant in TPS-MFC nanocomposites prepared by solution casting. As expected, cellulose nanofibers derived from husks and corncobs increased the Young's modulus and tensile strength of TPS films due to the strong interactions between the starch matrix and the high aspect ratio nanofibers. It was also noticed that mechanical properties could be further improved by the application of GMS surfactant.

J Polym Environ (2012) 20:404–411
DOI 10.1007/s10924-011-0380-7

ORIGINAL PAPER

Cell Wall Morphology, Chemical and Thermal Analysis of Cultivated Pineapple Leaf Fibres for Industrial Applications

W. O. Wan Nadirah · M. Jawaid · Abeer A. Al Masri · H. P. S. Abdul Khalil · S. S. Suhaily · A. R. Mohamed

Published online: 12 November 2011

Abstract A study on chemical, morphology, and thermal analysis of cultivated pineapple leaf fibres (PALF) were carried out. The chemical compositions were determined by using Technical Association Pulp and Paper Industries standards. Fourier Transform-Infrared Spectroscopy analysis of PALF detect sharp band at 1,733 cm^{-1}, due to the absorption of carbonyl stretching of ester and carboxyl groups which is most abundant in pineapple leaf hemicelluloses. Cell wall ultra structure of PALF was studied by using Transmission electron microscopy. Transmission electron micrograph confirmed that cell wall structure of PALF consists of middle lamella, primary wall and secondary wall including S_1, S_2 and S_3 layers. X-Ray Diffraction indicated that PALF have crystalline nature. Thermal analysis of PALF shows that $T_{10\%}$ and $T_{50\%}$ weight loss occurred at temperature of 212 and 306 °C respectively. Differential Scanning Calorimetry of PALF showed the broad endothermic peak at a temperature of 80 °C. The relationships between these properties were discussed and relate it with industrial application of pineapple leaf fibers.

Keywords Pineapple leaf fibres (PALF) · Chemical analysis · Cell wall · Thermal properties

W. O. Wan Nadirah · M. Jawaid · H. P. S. Abdul Khalil (✉)
School of Industrial Technology, Universiti Sains Malaysia, 11800 Penang, Malaysia
e-mail: akhalilhps@gmail.com

A. A. Al Masri
College of Medicine, King Saud University, Riyadh 11451, Saudi Arabia

S. S. Suhaily · A. R. Mohamed
Product Design Department, School of Arts, Universiti Sains Malaysia, 11800 Penang, Malaysia

Introduction

The high demand of wood products from day to day life due to population's growth indicated that recent wood scarcity is unable to fulfill people demand, and wood is no longer relevant and it required to replaced by an alternatives sources such as natural fibres. Natural fibres have the compositions, properties, and structure that make them suitable for fabrication of composite, textile, pulp and paper. The common natural fibres include flex, hemp, jute, kenaf, bamboo, sisal, and cotton. Within that mixed portfolio, pineapple leaves are one of the important natural resources which can be a principal source for fibres, chemicals and other industrial products [1]. Pineapple leaf fibres (PALF) are waste products from pineapple plant cultivation (Fig. 1). The pineapple, *Ananas comosus* (Fig. 2) belonged to the family *Bromeliaceae* is a short tropical herbaceous perennial plant with a 1–2 m for height and width [2]. According to FAO database online [3], Malaysia's production of pineapple leaf is about 384,673 metric tones for year 2008. Thus, it showed that pineapple leaf is annually renewable and available in abundance for industrial purpose without any additional cost since it is a residue product [4].

The PALF is a green long, thin, waxy and pointed with sharp spines on the edges as well as curved towards the cross section to maintain the stiffness of the leaf [5]. They also reported that PALF are white, creamy, and lustrous as silk and it has a softer surface than other vegetable fibre and has the ability to absorb and retain a good colour. Thus, the remarkable qualities of thinness, smoothness as well as pliability paper will be produced. Pineapple leaves have fine silky, medium length fibre with high tensile strength [6]. PALF is very hygroscopic, relatively inexpensive, an important natural fibre that exhibits high specific strength and stiffness [7].

nanotechnological applications [34]. In an another interesting work, researchers produced nanocellulose and its composites and confirmed that it is very versatile material having the wide range of medical applications, including cardiovascular implants, scaffolds for tissue engineering, repair of articular cartilage, vascular grafts, urethral catheters, mammary prostheses, penile prostheses, adhesion barriers and artificial skin [35].

Conclusions

The above studies can be summarized as follows:

1. PALF contained 74.33% of cellulose as promising in producing better pulp and paper manufacture. Besides, low lignin content (10.41%) allows these fibres undergo bleaching easily in paper processing.
2. Transmission electron microscopy has confirmed that cell wall structure of PALF consists of middle lamella, primary wall and thick secondary wall. Thick cell wall probably yielding higher rigidity index in pulp and paper field.
3. Percentage of crystallinity from XRD study was come out as 13.74% thereby had proved PALF have crystalline nature.
4. The chemical constituents degradation observed in TGA curve of pineapple leaves at temperature of 212 and 306 °C were $T_{10\%}$ and $T_{50\%}$ weight loss occurred respectively. Besides, melting temperature around 290 °C illustrated in DSC curve of PALF.
5. Based on morphological characteristics, thermal, and crystalline properties of pineapple leaves, it has the potentials to use as raw material in composite fabrication, and paper manufacturing.
6. Nanocomposites and nano cellulose from PALF are versatile materials for medical, and nanotechnological applications.

Acknowledgement The researchers would like to thank the Universiti Sains Malaysia, Penang for providing the Research Universiti (RU) Grant (1001/PTEKIND/814133) that has made this work possible.

References

1. Reddy N, Yang Y (2005) Trends Biotechnol 23:22
2. Tran AV (2006) Ind Crop Prod 24:66
3. FAO (Food and Agriculture Organization of the United Nations) Statistical Database (FAOSTAT) (2008) [Online]. http://www.fao.org. Accessed 6 July 2011
4. Munirah M, Rahmat AR, Hassan A (2007) Characterization and treatments of pineapple leaf fibre. Department of Polymer Engineering, Faculty of Chemical and Natural Resources Engineering, Malaysia Technology University, Johor Bharu
5. Bartholomew DP, Paull RE, Rohrbach KG (2003) The pineapple: botany, production and use. CABI Publishing, Wellingford, UK
6. Py C, Lacoeuilhe JJ, Teisson C (1987) The pineapple: cultivation and uses. Maisonneuve & Larose, Quae
7. Cherian BM, Leao AL, de Souza SF, Thomas S, Pothan LA, Kottaisamy M (2010) Carbohydr. Polym 81:720
8. Uma Devi L, Bhagawan SS, Thomas S (1997) J Appl Polym Sci 64:1739
9. Chollakup R, Tantatherdtam R, Ujjin S, Sriroth K (2010) J Appl Polym Sci 119:1952
10. Mishra S, Mohanty AK, Drzal LT, Misra M, Hinrichsen G (2004) J Macromol Mater Eng 289:955
11. Mukherjee PS, Satyanarayana KG (1986) J Mater Sci 21:51
12. Nieschlag HJ, Nelson GH, Wolff JA, Perdue RE (1960) Tappi 433:193
13. Panshin A, Dezeeuw C (1980) Textbook of wood technology, 4th edn. McGraw-Hill, New York
14. Abdul Khalil HPS, Siti Alwani M, Ridzuan R, Kamarudin H, Khairul A (2008) Polym Plast Technol 47:273
15. Abdul Khalil HPS, Siti Alwani M, Mohd Omar AK (2006) Cell wall of tropical fibers. BioResources 12:220
16. Wirawan R, Zainudin ES, Sapuan SM (2009) Sains Malays 38:531
17. Abdul Khalil HPS, Ireana Yusra AF, Bhat AH, Jawaid M (2010) Ind Crop Prod 31:113
18. Ververis C, Georghiou K, Christodoulakis N, Santas P, Santas R (2004) J Ind Crops Prod 19:245–254
19. Herbert Morrison W III, Akin DE, Archilbald DD, Dodd RB, Paul LR (1999) Ind Crops Prod 10:21–34
20. Mui ELK, Cheung WH, Lee VKC, McKay G (2008) Ind Eng Chem Res 47:5710–5722
21. Harada H, Cote WA Jr (1985) In: Higuchi T (ed) Biosynthesis and biodegradation of wood components. Academic Press, Orlando
22. Booker RE, Sell J (1998) Holz Roh Werstoff 56:1–8
23. Law KN, Jiang XF (2001) Tappi J 841:95
24. Ramiah MV (1970) J Appl Polym Sci 14:1323
25. Stout HP, Jenkins JA (1955) Ann Text Belg 4:231
26. Siregar JP, Mohd SS, Rahman MZ, Dahlan KZ (2011) Pertanika J Sci Technol 191:161
27. Akita K, Kase MJ (1967) Polym Sci A I 5:833
28. Remiro PM, Cortazar M, Calahorra E, Calafel M (2002) Polym Degrad Stab 78:83
29. Chu NJ (1970) J Appl Polym Sci 14:3129
30. Lopattananon N, Panawarangkul K, Sahakaro K, Ellis B (2006) J Appl Polym Sci 102:1974
31. Pineapple Paper Furniture by Yothaka (2008) [Online]. http://inhabitat.com/pineapple-paper-furniture-by-yothaka/. Accessed 2 Oct 2011
32. Banik S, Dey SK, Nag D (2011) Indian J Fibre Text 36:172
33. Leao AL, Souza SF, Cherian BM, Frollini E, Thomas S, Pothan LA, Kottaisamy M (2010) Mol Cryst Liq Cryst 522:318
34. Abraham E, Deepa B, Pothana LA, Jacob M, Thomas S, Cvelbard U, Anandjiwala R (2011) Carbohydr Polym 86:1468
35. Cherian BM, Leão AL, de Souza SF, Costa LMM, de Olyveira GM, Kottaisamy M, Nagarajan ER, Thomas S (2011) Carbohydr Polym 86:1790